Review #1 by John E. Walsh

This paper shows that the Bering Sea was a major contributor to the increased amplitude of the seasonal cycle of pan-Arctic ice extent in the first decade of the 21st century. Perhaps more importantly, it addresses a topic that is in need of further understanding: the variability of Bering Sea ice extent over decadal timescales. While the paper contains some interesting results, it comes up short in two respects: (1) recent events have passed it by, and (2) the explanation of the Bering's decadal variations is largely speculative.

With regard to (1), the paper's analysis ends in 2015. Since 2015, the Bering Sea has been the region of perhaps the most remarkable extremes of sea ice extent in the historical record: the extreme minima of 2018 and 2019. Bering ice extents during these two winters were only about 50% of the previous minima of the satellite era. This represents a spectacular reversal from the positive anomalies of 2008-2013 that shape the results and conclusions of the present paper. The recent extreme minima have put the Bering at the forefront of climate discussions. There are obvious implications for the Bering Sea ice trends highlighted in Figure 1 and elsewhere in the paper. As a result, the paper is seriously dated before it even gets into the publication process.

Reply: Thank you for reminding us of this important information! We followed your advice and updated all the available datasets to present: (1) NSIDC monthly sea ice concentration data from November 1978 to June 2019; (2) ECMWF ERA-interim meteorological fields data from January 1979 to April 2019; (3) ECMWF ORA-S4 ocean fields data from January 1958 to December 2017; (4) JISAO PDO index from January 1900 to September 2018; (5) NCEP GODAS ocean assimilation data from January 1980 to May 2019; (6) HadEN4.2.1 g10 ocean subsurface analyses data from January 1950 to December 2018; (7) WHOI OAflux data from January 1958 to December 2018. To probe into the physical mechanism related to the sea ice change, we also downloaded the NPGO index constructed by Di Lorenzo from January 1950 to December 2018. All above changes are described in the revised paper Section 2.

Once total Arctic sea ice extent time series is extended to the latest, its seasonal variation magnitude seems drop down again. That is, 2013-2018 annual standard deviation is overall lower than that of 2007-2012, representing a flavor of decadal scale oscillation feature (Fig. 1a). Fig. 1b shows the standard deviation differences for each month. It is obvious that discrepancies between the three periods (2007-2012 minus 1979-2006, and 2013-2018 minus 2007-2012) are primarily come from the summer (Aug-Oct, peak in Sep) and spring (Mar-May, peak in April) seasons. The spatial patterns further show that the Pacific section including the Chukchi sea and the Bering Sea (gray fan) as well as the Laptev and eastern Siberian seas is the major contributor to these decadal changes of total

Arctic sea ice extent (Fig. 1c & d). The normalized Chukchi-Bering SIE indices in ASO and MAM (Fig. 2) both exhibit abrupt change since 2007. In summer this change can be viewed as a mean state mutation or regime shift (Fig. 2a), while in spring it is more like a decadal oscillation (Fig. 2b). It seems that the annual cycle of total Arctic sea ice extent increases because of the persistent ASO Chukchi-Bering SIE retreat over the 2007-2018, while the increased decadal variability in MAM contributed to a strengthening of the seasonal cycle 2007-2012 relative to 2013-2018.

We made these revisions in the section 3.1 of the revised manuscript.

(2) The explanation for the Bering Sea ice history, especially its decadal-scale variability, leaves the reader wondering about the value added. The authors show that there has been a cooling of the Bering Sea at depth, coincident with the 2008-2013 positive sea ice anomalies, and that the water temperatures generally correlate well with the Bering ice extent over the entire record. But the reasons for the water temperature variations are only discussed speculatively: there is mention of Bering Strait throughflow (p6, lines 12-21) and atmospheric circulation variations (p5 bottom - p6 top), but there is no rigorous analysis. The text does not even indicate whether there was an increase in the heat exported through Bering Strait in the 2007-2008 timeframe, nor whether there would be a compensating inflow of heat from the south. The hypothesis about changes in ocean currents and Ekman pumping is also not supported by hard evidence, as no ocean current data were included in the analysis. The linkage between ice extent and water temperature does not distinguish cause and effect, and even the possible linkage with the PDO is rather murky in view of the lead-lag correlation in Figure 3d. In short, the paper does not provide a compelling explanation for the Bering Sea winter/spring ice expansion of 2008-2013 (let alone the spectacular abrupt decrease in 2018 and 2019).

Reply: Thank you for your suggestions! As we noted in the original manuscript, the spring Bering Sea ice high index is associated a SLP dipole pattern prior-2007 but an anomalous high pressure thereafter. Furthermore, the anomalous Bering SST anomalies exhibits a close connection with North Pacific large-scale SST pattern in the recent decade, in great contrast to the isolated Bering SST variability before 2007. In addition, the SST anomalies extend down to the subsurface after 2007. This remarkable pattern change suggests that the spring Bering Sea ice variability is getting predominated by the ocean dynamical processes in Pacific.

The extra-tropical North Pacific climate variability is dominated by two decadal-scale ocean-atmosphere modes, the Pacific Decadal Oscillation (PDO) and the North Pacific Gyre Oscillation (NPGO). Further analyses reveals that the NPGO pattern exhibits great decadal change and becomes phase-lock with PDO in the post-2007 period. The effects of PDO and NPGO on the Bering Sea temperature anomalies as well as the associated dynamical processes were

explored. It is the NPGO change and its synchronization with the PDO that trigger the recent decadal oscillation of Bering Sea ice extent. This notable decadal oscillation in the Bering sea plays an important role to interpret recent total Arctic sea ice extent change. In the background of global warming and polar amplification, the total Arctic ice volume and thickness decrease persistently. It is conceivable that the future change of Arctic sea ice extent is more sensitive to the complicated air-sea coupling processes. Therefore, to better understand and predict the future Arctic sea ice change, we should pay more attention to these large-scale coupled modes such as Pacific decadal variability and Atlantic multi-decadal oscillation.

The detailed physical mechanisms that account for the decadal oscillation of spring Bering Sea ice extent is presented in the revised manuscript section 3.2-3.4.

Some specific comments:

1. Page 1, line 19: The decrease of pan-Arctic ice extent in recent decades has not really been "continuous", as there have been ups and downs associated with interannual variability. One can also question the statement in line 20 that the "rate of ice loss accelerates from the 1990s". If one calculates the trend of pan-Arctic September ice extent for the 2007-2018 period, the trend is essentially zero.

Reply: Some expressions were imprecise. We corrected them in the new manuscript. Thank you for pointing this out! The revision made in Page 1, line 24-25: "Arctic sea ice has declined along with the Arctic amplification of global warming. It is noteworthy that the remarkable ice retreat from the late 1990s".

2. Page 1, line 32: Not a sentence.

Reply: revised.

3. Page 4, line 32-33: In another example of the dated nature of the study, the PDO has been positive for nearly the entire period since 2015.

Reply: Thank you for reminding us about this! We extend our analysis period and reveal close linkage between the phase change of PDO and NPGO and the decadal oscillation of Bering Sea ice. Details please see the reply to your main point 2.

4. Page 6, lines 1-4: Figure 7 needs some elaboration, including an explanation of how Ekman pumping contributes to the proposed linkage between the atmosphere and the Bering Sea water temperatures and sea ice. In particular, what happens dynamically when Ekman pumping changes from negative to positive? What causes the sign reversal, and how do upwelling and downwelling relate to changes in water temperature? In other words, please present more information on the mechanistic linkage alluded to here.

Reply: We agree with your viewpoint and explore the detailed oceanic physical response to the atmospheric forcing in the revised manuscript. Details please see

the reply to your main points.

5. Page 6, lines 22-31: There should be some description of the NPO and NPO-NPGO, and some supporting references. As it now stands, the NPO and NPGO seem to appear out of the blue.
Reply: Thank you so much for providing these clues! According to your suggestions, we compared the roles played by the PDO and NPGO in the Bering sea ice decadal changes and relevant physical processes. The conclusion is made that the NPGO changes and its synchronization with PDO mode may trigger the decadal change of Bering Sea. Details please see the reply to your main points.

Review #2

This paper presents an analysis of Bering and Chukchi Sea ice, showing contrasting decadal variability with decreases in the summer-autumn and increases in the winter-spring. Sea ice, atmospheric reanalysis, and ocean temperatures and velocities are examined to explain this behavior. The authors find that the pattern is likely due to subsurface cooling in the northern Bering Sea.

General comment

Overall, this is well-written paper and the analysis is competent. However, I have a few notable issues, listed below. The second issue in particular is critical and is the major reason for the decision of Major Revision.

1. The authors generally treat the Bering and the Chukchi Seas as one system, but I'm not sure if this really appropriate. For example, they say that the B-C shows decreases in the summer-autumn and increases in the winter-spring. However, the Bering is ice-free during summer-autumn, so the decrease is in the Chukchi, not really the B-C. Similarly, the Chukchi is completely ice-covered during winter-spring, so the increase there is really in the Bering, not the B-C.

During the analysis, they do start to treat the two more separately, but their approach is generally that these are two closely inter-connected systems and I'm not convinced that this is the case. There is indeed connection through the Bering Strait, and though that is narrow and shallow, there has been much research demonstrating that inflow of warm Pacific waters has contributed to summer ice loss in the Chukchi. But the Chukchi is also connected to the rest of the Arctic Ocean, particularly the neighboring seas — the Beaufort and the East Siberian. For example, the Beaufort Gyre circulation transports ice into the Chukchi and much of that ice is thicker, multi-year ice. This aspect seems to be ignored in the

paper- particularly the role of changes in multi-year ice, which has been rather dramatic in recent years.

And while the Bering influences the Chukchi, I don't think the reverse is generally true – the ocean waters flow into the Chukchi. There can be some sea ice outflow, but this is pretty rare and ephemeral. So when talking about the B-C, it's really more of a one-way street, not an interacting system. The main connection would be through the atmosphere where circulation patterns can affect the transport of heat, etc. between the two regions.

Maybe this is more semantics on my part. In the body of the paper, the authors seem to be clearer and focus more on the Bering Sea and then interaction with the Arctic Ocean in general. So maybe some changes in phrasing in places would help here.

Reply: We very much agree that the Chukchi Sea ice and Bering Sea ice vary in different seasons and under the different mechanisms. We apply the term of ChukBerSIE in order to stress that the abrupt change of total Arctic sea ice extent variance is originated from this Pacific sector, rather than other Arctic areas. We recognize that the summer Chukchi sea ice variability is closely connected to the inner Arctic Ocean processes, but the spring Bering Sea ice is more under the spell of local climate variability. While much attention is paid to the drastic summer Arctic ice cover reduction, few people care about the spring Bering sea ice variability. Our preliminary analysis reveals that the Bering Sea ice has experienced a strengthening decadal oscillation, which at least partly accounts for the abrupt change of total Arctic sea ice variance in the recent decade. However, we did not know the detailed processes that trigger this decadal oscillation of Bering Sea ice. This is the motivation of our study.

We greatly appreciate your suggestion about the phrasing change, and we do some revision to specify the difference between the Chukchi and Bering regions in Page 4 Line 26-27: "though the sea ice variations in the Chukchi Sea and the Bering Sea are probably subject to different dynamical processes and thermal conditions". And we further show and compare the difference between the summer Chukchi sea ice and spring Bering Sea ice in Page 4 Line 28- Page 5 Line 4 (Fig. 2).

2. The other main issue is, unfortunately, the timing of this paper. As the authors are probably aware, the situation in the Bering has completely reversed over the last two winters. Both 2017-2018 and 2018-2019 were record or near-record lows over most of the winter-spring. I recognize that things can change and that papers have to be published at some point and new data will come in after submission. However, this paper stops with 2015, so after the last two winter-springs, it feels particularly out date… Even without updated ocean data, at least some of the analysis could be updated.

Because the change is so substantial, I feel the authors should really redo the analysis through at least 2018. As noted above, I recognize that at some point, analysis has to stop and a manuscript must be prepared and submitted. But this paper just feels too out of date to be particularly relevant. At the very least, if the authors can't update their analysis, they should thoroughly discuss the recent changes in the Bering Sea ice cover and the implications for their study.

Reply: Thank you! We follow your suggestion to extend all the datasets to the latest time except for the ORA-S4. This dataset ends up in dec2017. Please refer to the reply to review 1 for the detailed data description. We then redo the analyses using the new datasets and make much more revisions on our conclusions and physical interpretation.

3. Overall, the analysis is rather cursory. The authors pull together the right datasets and the analysis that they do is reasonable. But it doesn't seem enough to really substantiate their hypotheses – particularly in light of #2 above. The paper is <6 pages long and while I enjoy short, concise papers, the analyses are not very deep and they don't dig into the data enough to definitively support their conclusions.

Reply: Thank you for your insightful comments! In the revised manuscript, we explore in detail the physical factors that trigger the recent Bering Sea ice change. We finally conclude that the NPGO mode change and its synchronization with the PDO in the recent decade are the principle cause for the decadal oscillation of Bering Sea ice. Detailed statistical and physical analyses are now included in the paper.

4. The final issue is several grammar errors—not major, but occasionally throughout the manuscript. Some are note below in Minor Comments, but a thorough proofreading for English grammar would be helpful.

Reply: Thank you for your careful check-up! The revised manuscript is thoroughly proofread for English grammar.

Specific comments

5. 16-17: "significant" and "insignificant" are each used. Do these refer to statistical significance? If so, the significance level should be specified. If not, then I would suggest different wording, e. g., substantial, notable, etc. to avoid confusion over the use of "significant".

Reply: Thank you! Yes, these refer to statistical significance with the confidence level of 95%. Revised.

Figure 1b: I find this figure a bit confusing. The 120W-60W is not labeled—that's the Canadian Archipelago. I recognize this isn't terribly relevant to the study, but odd to have just that longitude range unlabeled. More relevant though is: where is the Laptev? I think it's included in what is labeled "East Siberian" –if so, that should be noted. Maybe what would help is a map that has the seas labeled and the longitude boundaries outlined.

Reply: We make much revision on all the figures. In the new version, we emphasize the decadal differences of Arctic sea ice variance. And we outlined the Chukchi-Bering section as the key region of this decadal change. Details can be found in the reply to review 1.

Minor Comments

1, 9: "in recent decade"—a minor grammar issue, but it makes things ambiguous: is it "in the recent decade", or is it "in recent decades"? This is repeated elsewhere in the manuscript as well.

Reply: It should be "in the recent decade". Corrected. Thank you!

1, 27: "transit" should be "transition"

Reply: revised in Page2 Line 1, thank you!

2, 10: "urgent" not "urgently"

Reply: revised in Page 2 Line 21.

5, 22: "decline" not "descent"

Reply: revised.

6, 15: as noted above, I don't think you can any longer say "lengthening sea ice seasons" for the Bering—certainly not for the last two years.

Reply: Thank you! Revised in Page 11 Line 28- Page 12 Line 1: "Echoing to this increasing heat flux… lead to the recent Arctic climate change".

6, 29: In light of the last two years' worth of data, I think the question of whether the "amplifying seasonal cycle of Arctic sea ice cover will be sustained" has been answered, at least in terms of the Bering Sea: no!

Reply: Thank you! We revised it. It is not "amplifying" but "decadal oscillation".

The ~~recent amplifying seasonal cycle of the~~ Arctic sea ice extent change connected~~related~~ to ~~the subsurface cooling in the Bering Sea~~Pacific decadal variability

Xiao-Yi Yang[1, 2] ~~, and~~ GuiHua Wang[3~~2~~], and Noel Keenlyside[4]

[1]State Key Laboratory of Marine Environmental Science, and College of Ocean and Earth Sciences, Xiamen University, Xiamen China.

[2] Southern Marine Science and Engineering Guangdong Laboratory (Zhuhai), Zhuhai China

[3~~2~~] Department of Atmospheric and Oceanic Sciences &Institute of Atmospheric Sciences, Fudan University, Shanghai China

[4] Geophysical Institute, University of Bergen, Bergen Norway

Correspondence to: Xiao-Yi Yang (xyyang@xmu.edu.cn)

Abstract. After an unprecedented ~~and accelerated~~ retreat, the total Arctic sea ice cover for the post-2007 period~~in recent decade~~ is characterized ~~with~~ by low extent and ~~large amplitude of~~a remarkable increase in annual cycle amplitude. We have identified the leading role of spring Bering Sea ice in explaining the changes in the amplitude of ~~This study investigated the spatial temporal variation of the Arctic sea ice extent and the potential factors accounting for its amplifying~~ the ~~seasonal~~ annual cycle of total Arctic sea ice. In particular, these changes are related to the recent occurrence of multi-year variability in spring Bering Sea ice extent. This is due to the phase-locking of the North Pacific Gyre Oscillation (NPGO) and the Pacific Decadal Oscillation (PDO) after about 2007, with a correlation coefficient reaching -0.6. Furthermore, there emerge notable changes in the sea level pressure and sea surface temperature patterns associated with the NPGO in the recent decade. After 2007, the NPGO is related to a quadrupole SLP anomalies that is associated with the wind stress curl and Ekman pumping rate anomalies in the Bering deep basin; these account for the change in Bering Sea subsurface variability that contribute to the decadal oscillation of the spring Bering Sea ice extent. ~~The results show that the Chukchi Bering sector of Arctic exhibits a contrasting decadal variation of sea ice extent between the~~

~~different seasons: The sea ice in recent decade decreased in summer autumn seasons but increased significantly in spring, leading an amplifying seasonal cycle. This decadal expansion of spring Chukchi Bering sea ice may be attributed to the significant subsurface cooling in the northern Bering Sea.~~

1 Introduction

The Arctic sea ice cover is an integral part of the Arctic climate system as well as one of the strongest~~most effective~~ indicators to the global climate change. Since the satellite era, the Arctic sea ice has ~~experienced a continuous~~ declined along with the Arctic amplification of global warming. It is noteworthy that the ~~rate of~~remarkable ice ~~loss accelerates~~retreat from the late 1990s (Comiso et al., 2008; Comiso, 2012; Stroeve et al., 2012)~~, in correspondence to~~ and the ~~abrupt rising of~~associated Arctic surface ~~air temperature~~warming (Screen and Simonds 2010)~~. This~~ is in great contrast to the simultaneous slowdown of surface warming in the Northern Hemisphere extra-polar regions (Cohen et al., 2014). Therefore the possibility of "tipping points" or abrupt changes in the Arctic climate system has come to be a subject of much debate (Lindsay and Zhang, 2005; Lenton et al., 2008; Eisenman and Wettlaufer, 2009; Armour et al., 2011; Serreze, 2011; Tietsche et al., 2011; Duarte et al., 2012; Bathiany et al., 2016a). ~~Their controversy lies in~~There are two aspects to the controversy: 1. Whether or not the Arctic sea ice cover will melt persistently and irreversibly to an ice-free state; 2. Whether or not a bifurcation with multiple steady states exists such that the Arctic may transition from perennial to seasonal ice cover. In general, ~~the~~ model ~~simulation~~ studies ~~defied~~ do not support the existence of threshold or "tipping point" behaviour. By ~~modulating~~ prescribing atmospheric carbon dioxide, Armour et al. (2011) and Bathiany et al. (2016a) demonstrated that there is neither irreversibility nor multiple states for the total Arctic sea ice cover. Tietsche et al. (2011) further proposed a recovery mechanism for Arctic summer sea ice based on the anomalous long-wave emission and atmospheric heat advection. Nevertheless, ~~the data~~ statistical ~~researches~~ analysis of observations present~~ed~~ various early warning signals ~~for an~~of abrupt Arctic climate change. For example, Duarte et al. (2012) argued that it is the ice thickness rather than ice extent that cannot be rebuilt. With the persistent thinning of Arctic sea ice, open-water formation increase during the melting season is probably followed with higher efficiency of ice production during the next ice growth season through the ice thickness-ice growth feedback (Barnhart et al., 2016). Massonnet et al. (2018) further suggested that the reductions

in ice thickness may lead to enhanced seasonality but decreased interannual variability and persistence of the Arctic sea ice extent. Livina and Lenton (2013), by the "potential analysis", detected the abrupt and persistent increase in the seasonal cycle of Arctic sea ice cover since 2007. Therefore, the dramatic climate change in Arctic sea ice is much more pronounced in the amplitude of the seasonal cycle than in the annual mean ice area.

While previous studies mostly ~~detected~~ considered the signal of abrupt Arctic climate change in terms of fast sea ice decline and the amplifying seasonal cycle, few of them ~~noted~~ focused on the regional and seasonal dependence of Arctic sea ice variation. ~~Recently,~~ Close et al. (2015) ~~examined~~ concluded that the ~~timing of~~ onset of Arctic sea ice decline ~~and concluded that~~is much earlier ~~onset time~~ and ~~weaker~~ the post-onset rate of loss is weaker ~~occurred~~ in the Pacific ~~sector~~ than in the Atlantic sector. Onarheim et al. (2018) noted the distinct transformation of seasonal sea ice variability in various Arctic regional seas and predicted their different ice-free period. These~~is~~ results indicate~~s~~ that Arctic sea ice variations are~~is~~ asymmetrical and strongly dependent on the local physical process, resulting in the complexity and difficulty in predicting the future Arctic climate change. Therefore, we need to probe into the recent Arctic sea ice variability, ~~in detail~~ both temporally and spatially. ~~More~~ It is urgent~~ly is~~ to ~~explore~~ understand the physical mechanisms accounting for the recent amplifying seasonal cycle of Arctic sea ice cover, so as to better ~~understand~~foresee future ~~the~~ Arctic climate change. ~~and improve the predictability of climate change.~~

2 Data and methods

We used the ~~M~~monthly sea ice concentration dataset ~~from 1979 to 2015~~that was developed by the National Aeronautics and Space Administration team using the *Nimbus*-7 SMMR (1978-87), DMSP SSM/I (1987-2009), and DMSP SSMIS (2008-present) satellite passive microwave radiances on a 25km ×25km polar stereographic grid (Cavalieri et al., 2013); and can be freely downloaded from National Snow and Ice Data Center (NSIDC) website. The sea ice extent (SIE) was generated from Nov1978 to Jun2019 by summing the areas of the concerning grid boxes covered with at least 15% ice concentration.

We also used~~The meteorological variables including~~ surface air temperature, sea level pressure, 850hPa zonal and meridional winds, and sea surface temperature ~~were obtained~~ from the European Centre for Medium-Range Weather Forcasts (ECMWF) ERA-interim reanalysis dataset (Dee et al., 2011), with a horizontal resolution of 0.75 °×0.75 °and ranging from Jan1979 to Dec2018~~5~~.

The ORAS4 ocean temperature and horizontal velocity data was used to examine the ocean subsurface variability. The ORAS4 is a newly-released version of ECMWF ocean reanalysis dataset, which is based on the NEMO ocean model and assimilates the available temperature and salinity profiles and sea-level anomalies through the NEMOVAR assimilation scheme (Balmaseda et al., 2012). The dataset spans the period of Jan1958 to Dec2017~~5~~, with the resolution of 1 °× 1 °grid horizontally and 42 levels vertically.

We used two~~The~~ monthly climate indices: The Pacific Decadal Oscillation (PDO) index, ~~was~~ downloaded via JISAO website at http://research.jisao.washington.edu/pdo/~~.~~; and The North Pacific Gyre Oscillation (NPGO) index, constructed by Emanuele Di Lorenzo (Di Lorenzo et al., 2008) and downloaded from http://www.o3d.org/npgo/.

The NCEP Global Ocean Data Assimilation System (GODAS) data, HadISST1 sea surface temperature data and the Hadley Centre EN4 quality controlled ocean data were also used to validate the results.

The WHOI Objectively Analyzed Air-Sea Fluxes (OAflux) surface turbulence heat flux data from Jan1958 to Dec2018 was also applied in this study. The spatial resolution is 1 °×1 °. The OAflux dataset is constructed from multiple data sources, an optimal blending of satellite retrievals and reanalyses data (Yu et al., 2008).

~~All the anomaly data was obtained by subtracting the climatological mean of 1979-1998. The running trends were estimated by applying the least square method on a moving 11-year window. The significance testing of decadal trend is at the 95% confidence level taking into account its temporal autocorrelation (Santer et al., 2000).~~

The amplitude of seasonal cycle is estimated by calculating the annual standard deviation based on the following formula:

$$\sigma_j = \sqrt{\sum_{i=1}^{12} (x_{ij} - \overline{x}_j)^2} \quad \mathrm{std}_j = \sqrt{\frac{1}{12}\sum_{i=1}^{12} (x_{ij} - \overline{x}_j)^2}$$

where the subscripts of i, j are the month and the year, respectively. The overbar denotes the annual mean.

The multi-year averaged monthly standard deviation is computed as:

$$\mathrm{std}_i = \sqrt{\frac{1}{n}\sum_{j=1}^{n}\left(x_{ij} - \overline{x}_j\right)^2}$$

where n denotes the number of years for averaging.

A harmonic analysis method based on fast Fourier transform is used to extract the decadal component of the spring Bering sea ice index, and the PDO and NPGO indices.

~~Zonal mean ocean temperature anomalies with PDO removed are computed by following steps: First regressing the zonal mean temperature onto the PDO index. Then the PDO congruent temperature anomalies are obtained by multiplying the regression coefficients with the PDO index. Finally, this PDO congruent part is subtracted from the original zonal mean temperature anomalies.~~

3 Results

3.1 ~~Amplified seasonal cycle~~Decadal change of ~~the~~ Arctic sea ice extent variance

The time series of monthly total Arctic SIE anomalies from ~~Jan~~November 1978~~9~~ to ~~dec~~2015 June 2019 is shown in Fig. 1a (upper panel), in parallel with the ~~annual cycle~~ magnitude~~s~~ of the annual standard deviation (lower panel in Fig. 1a). The total Arctic sea ice cover variability during the satellite period goes through three distinct stages: relative high extension and ~~steadiness of~~stable sea ice cover during 1979-1998; ~~the~~ fast ice retreat period from 1999 to 2006; and the lower ice extension and level-off of ice retreat trend ~~in~~ post-2007~~. period.~~ During the 1999-2006 period sea ice declines~~After the persistent and dramatic decline period~~ with a dramatic rate of ~~about~~ over -0.13~~127~~ million km^2/year ~~from 1999 to 2006~~, such that the climatology of total Arctic sea ice extent drop~~sped down remarkably~~ from ~~12.2~~13 million km^2 for the 1979-1998 period to ~11.6~~3~~ million km^2 for the post-2007 period. In association with the slow-down of Arctic sea ice retreat there is an~~the~~ abrupt ~~increasing~~ increase in the magnitude of annual ice fluctuation~~s around the climatological mean~~ in the recent decade. ~~Actually~~ In particular, the mean value of annual standard deviation leap~~sed~~ from 3.26~~0.25~~ million km^2 before 2007 up to 3.79 ~~0.56~~million km^2 ~~after the year of~~in the period of 2007-2012. Thereafter the mean annual standard deviation drops down again to 3.54 million km^2 in 2013-2018. Therefore, the current state of Arctic sea ice cover~~in recent decade~~ is characterized by the lower coverage, ~~the~~ a level-off in the linear decline trend, and an~~the~~ intensi~~fication~~~~ve~~ of the seasonal cycle.~~fluctuation.~~ All these signals herald the transition to another~~of~~ Arctic climate regime, which is a~~one of the~~ hot topic~~s~~ in the climate research community (Livina and Lenton 2013; Bathiany et al., 2016b)

In view of the strong ~~seasonality and localization of~~changes in Arctic sea ice seasonality~~variability~~, we further examine the decadal changes of sea ice extent between the three periods (i.e., 1979-2006, 2007-2012 and 2013-2018) for different calendar months (Fig. 1b). From the definition of multi-year averaged standard deviation depicted in Section 2, monthly deviations from the annual mean are squared and averaged for the separate three periods. The square roots are taken and the differences between the first two periods (black line) and the last two periods (red line) are estimated for each month. Both the increase in 2007-2012 and the decrease afterwards in the annual standard deviation are associated with the same bimodal change in standard deviation for different calendar months, with the main peak in September and the secondary peak in April-May. The spatial distribution of changes in the standard deviation of sea ice concentration is presented by calculating the sum of the absolute differences in the standard deviation in these two peak seasons (summer August-October mean and spring March-May mean; fig. 1c & d). There is a great contrast between the Pacific and the Atlantic sectors in both seasons: while the Pacific sector including the Bering Sea, the Chukchi Sea, the eastern Siberian Sea, the Laptev Sea and the Beaufort Sea contributes to the observed decadal changes of total Arctic sea ice extent (fig. 1a & b), the Atlantic sector including the Barents Sea, the Greenland Sea and the Baffin Bay offsets these changes. It is notable that the maximum variance changes are located in the north and south sides of the Bering Strait, i.e., the Chukchi Sea in summer and the Bering Sea in spring (labeled the ChukBer region, and demarked by the grey fan-shaped frame), following the seasonal advance and retreat of climatological sea ice extent. In addition, the climatological mean sea ice extent for three periods also exhibit decadal changes, with the 2007-2012 mean ice edge retreating to the northernmost in summer (fig. 1c green line) and extending to the southernmost in spring (fig. 1d green line); this is consistent with changes in annual standard deviation (fig 1a, bottom). Thus, the ChukBer region plays a key role in the recent change in Arctic sea ice seasonality and variability, though the sea ice variations in the Chukchi Sea and the Bering Sea are probably subject to different dynamical processes and thermal conditions.

~~probed into the fine structure of ice regime shift by contrasting the differences of meridional ice extent between the 2007-2015 mean and the 1979-1998 mean in a month–longitude section (Fig. 1b). The Atlantic sector including Baffin Bay, Greenland Sea and Barents and Kara seas exhibits uniform and season-independent descents of sea ice extent. In contrast, the sea ice extent in the Pacific sector decreased in summer-fall season but increased in winter-spring season in recent decade. This seasonality is extraordinarily evident in the Chukchi-Bering (ChukBer) seas, where the SIE annual standard~~

~~deviation goes through a sharp rise of ~0.24 million sq. km in the last decade by reference to the period of 1979-1998. The seasonality of the ChukBer SIE mean state change as shown in figure 1b recurs on the decadal time scale. The 10-yr running trend analysis of ChukBer SIE reveals the notable retreat in August-October and expansion in March-May since the early 2000s (Fig. 1c). The strong contrast of SIE decadal trends in the ChukBer region is partially offset by the uniformly accelerated ice retreat around the whole year in the Atlantic sector (Figure not shown), contributing to the recent amplifying seasonal cycle of total Arctic sea ice.~~

Fig. 2 shows the normalized ChukBer sea ice extent indices in summer and spring seasons. In summer the index represents variations in sea ice extent mainly in the Chukchi Sea, because of the seasonal retreat of sea ice; while in winter it represents variations in the Bering Sea. The summer Chukchi sea ice variability exhibited a tendency similar to the total Arctic sea ice variability: relative stable sea ice cover in early period, followed by a fast decline from the late 1990s to the early 21st century. After 2007, the Chukchi summer sea ice cover has remained in a low extent and leveling-off stage in the recent decade. The Bering Sea ice in spring, however, varied in a quite different pace. The apparent transition from a moderate interannual variability to decadal-scale variability with much larger magnitude emerged around 2007. The contrasting behavior is consistent with the changes annual standard deviation: anomalous high ice extension in spring and lower ice coverage in summer in the ChukBer region collaborate to the abrupt increase of seasonal cycle magnitude for the period of 2007-2012; thereafter, the spring Bering ice cover retreated remarkably, accounting for the retracement of total Arctic sea ice annual standard deviation for the period 2013-2018.

It is widely recognized that significant summertime ice loss in the Chukchi Sea is primarily attributed to (thermodynamic) ice-albedo positive feedback ~~thermodynamically~~ and (dynamic) strengthening transpolar drift ~~dynamically~~. So far there is a lack of comprehensive understanding and interpretation for the recent ~~expansion~~ decadal change of ~~ChukBer~~ Bering ice extent in spring~~, which is critical to intensification of Arctic sea ice annual cycle.~~ Therefore, a composite analysis is applied to various oceanic and atmospheric fields to explore the physical mechanism that triggered the decadal change of spring Bering Sea ice extent. ~~we constructed the normalized spring (March-May mean) ChukBer Sea ice extent index (SBII) as shown in Fig. 1d.~~ Based on the threshold of $\pm$0.7~~1~~ standard deviation of spring Bering sea ice extent index (SBII), a total of 1~~8~~5 out of ~~37~~40 years are selected to do the ~~following~~ composite analysis, including ~~8~~10 high index years (1984, 1992, 1994, 1995, 1999, 2008,

2009, 2010, 2012 and 2013) and 8~~7~~ low index years (1979, 1989, 1996, ~~2002,~~ 2003,~~ 2004,~~ 2015, 2016, 2017, 2018).

3.2 Abrupt transition of air-sea interaction in the Pacific sector

As the sea ice is sensitive to local thermal conditions in the ocean-atmosphere interface, the March-May mean surface air temperature, sea level pressure and 850hPa wind anomalies~~To interpret the abrupt change of total Arctic SIE prior- and post-2007 in terms of the climate change in the Bering Sea, various related physical variables~~ are composited based on SBII index (high index years minus low index years) in two periods of 1979-2006 (Fig. ~~2~~3 left panels) and 2007-201~~5~~8 (Fig. ~~2~~3 right panels). For both periods, the ~~anomalous expansion~~positive phase of SBII corresponds to the significant cooling (negative anomalies of surface air temperature) over the Bering area (Fig. 3~~2~~a & b~~d~~). However, the ~~surface heat flux,~~ SLP and 850hPa wind anomalies associated with the SBII present completely different patterns~~ for the two periods~~. In 1979-2006, the Chukchi-Bering region is dominated by the anomalous SLP dipole pattern and the attendant northerly winds in the lower troposphere (Fig. ~~2b~~3c). The cold advection in lower troposphere leads to the drop in local air temperature ~~drops accordingly, leading to intense heat loss over a broad area of north Pacific high latitudes~~ (Fig. 3a~~2e~~). In contrast to the early period, the spring ~~Bering Sea~~ ice expansion after 2007 is associated with a~~n~~ ~~in~~significant high SLP anomaly over the Bering Sea and the patchy northerly winds on its eastern flank (Fig. 3d~~2e~~), and these can hardly account for the broad cooling over the Bering region and the adjacent northeastern Pacific (Fig. 3b). ~~There is no apparent oceanic heat loss but significant reverse heat transfer from atmosphere to ocean over the ice-covered northern Bering Sea (Fig. 2f). We therefore speculated that the Bering Sea surface cooling rather than the overlying atmospheric process may be responsible for the spring ice cover expansion in recent decade.~~

The SBII-related March-May mean sea surface temperature and subsurface (165m) temperature anomalies are shown in Fig. 4. ~~To further verify the correspondence of SBII and the Bering Sea surface temperature, we compared the composite patterns of North Pacific SST anomalies on the SBII between the two periods (Fig. 3a).~~ For the early period, ~~T~~the positive SBII phase is associated with the local surface cooling that is confined in the Bering Sea area~~ for the early period~~. In the later period, however, the spring Bering ~~sea~~Sea ice expansion is connected to a large-scale SST anomaly pattern pattern:~~similar to Pacific Decadal Oscillation (PDO) mode, i.e.,~~ the significant cooling in the Bering Sea ~~can~~ extends

along the costal North America coast to the central tropical Pacific, sandwiching the warming anomalies in the adjacent area of the Kuroshio extension (Fig. 43b). In addition, cooling anomalies in the early period are mostly limited to the sea surface, while those in the later period extend to the subsurface layer (Fig. 4d).

To further assess the connection between the post-2007 SBII decadal change and local thermal conditions, the surface air temperature, surface sea temperature and subsurface temperature anomalies from various datasets are averaged in the Bering region (170-200 ℉, 55-65 ℕ, delimited by the grey rectangles shown in Fig. 4) and low-pass filtered by 13-month running mean. All the time series during the period of 1950-2018 are plotted in Fig. 5. The Bering mean air temperature shows moderate negative anomalies in 2007-2012 but remarkable warming afterwards (Fig. 5a). Although there are subtle differences in terms of magnitude and timing, the persistent cooling in about 2007-2012 and warming in recent five years are evident in all the SST and subsurface temperature data (Fig. 5b-f). This indicates that the recent SBII change may connect more to the large-scale oceanic dynamical processes or ocean-atmosphere coupling modes rather than to the local atmospheric circulation. Here we used all-month data instead of March-May mean because the seasonality in subsurface temperature is very weak and the post-2007 changes of subsurface temperature are prominent in all seasons. For the surface temperature, however, the seasonality is strong: the SST decadal oscillation can be detected in the winter and spring seasons, but obscured by a long-term warming trend in the summertime; the surface air temperature shows even weaker signals of decadal change in the cold seasons and stronger warming trends in the warm seasons (figures not shown).

~~We then examined the monthly PDO index and found the obvious phase shift from positive PDO to negative PDO in 2000s (Fig. 4). Many studies already noticed this Pacific climate regime shift and its connection with the recent global warming hiatus (Trenberth and Fasullo 2013; England et al., 2014). The time series of the spring (March-May mean) PDO index and the SBII are shown in Fig. 3c. There is significant negative correlation between the two indices, with the correlation coefficient of -0.47 during the whole period. Echoing the transition of North Pacific climate, an obvious decadal change appears in the correlation between the PDO and SBII. The correlation coefficient leaps up over -0.7 in the new century, in great contrast to zero correlation in the early two decades. The month-by-month correlation of PDO with SBII reveals that in the inter-annual time scale, the SBII lead PDO by 0~6 months (Fig. 3d). This to some extent rules out the possibility that the recent Bering Sea cooling is directly triggered by the~~

~~Pacific climate regime shift. In other words, the Bering Sea cooling may coincide with the recent phase switch of PDO.~~

3.3 NPGO pattern change and its synchronization with the PDO~~Subsurface cooling of the Bering Sea in recent decade~~

Numerous previous studies asserted that extra-tropical North Pacific climate variability is dominated by two decadal-scale ocean-atmosphere coupled modes: the Pacific Decadal Oscillation (PDO) (Mantua et al. 1997) and the North Pacific Gyre Oscillation (NPGO) (Di Lorenzo et al. 2008). Though defined independently as the first and second basin-scale EOF modes of sea surface temperature anomalies and sea surface height anomalies in the north Pacific Ocean respectively, the PDO and NPGO bear strong resemblance in their physical mechanisms and related climate anomalies. They are both forced by the El Niño-like tropical Pacific SSTA (Newman et al. 2003; Di Lorenzo et al. 2010), connected to the western Pacific Kuroshio-Oyashio extension through the ocean Rossby wave propagation (Schneider and Corneulle 2005; Ceballos et al. 2009), and impact the low-frequency variability of the marine ecosystem system (Miller et al. 2004; Di Lorenzo et al. 2013; Sydeman et al. 2013). Besides the remote tropical ENSO forcing, the PDO and NPGO can be driven by the local ocean-atmosphere interaction. The ocean, as a low-frequency filter, integrates the atmospheric stochastic noise and thereby contributing to the decadal-scale variability (Newman et al. 2016; Yi et al. 2015). The corresponding large-scale atmospheric modes are the Aleutian Low variability (for the PDO) and the North Pacific Oscillation (for the NPGO).

The large-scale Pacific SST anomaly pattern in the later period (Fig. 4b) alludes to the PDO and the NPGO as the candidates responsible for the decadal variations in the SBII during the most recent period. Therefore, changes in the spring (March-May mean) PDO and NPGO patterns are assessed by regressing the SST and SLP anomalies onto the two indices respectively for the different periods (Fig. 6). The PDO positive phase is associated with the deepening of Aleutian Low, warming in the northeast Pacific, including in the Gulf of Alaska and along the California coast, while there is cooling in the Kuroshio extension. Moderate warming in the eastern equatorial Pacific is discernable (Fig 6a). In the recent decade, however, the PDO-related SLP pattern is almost unchanged but the eastern Pacific warming enhances greatly. Notably the Bering Sea and the central equatorial Pacific stand out to be among the most significant warming regions (Fig 6c). The spring positive NPGO corresponds to an

anomalous high pressure over the most of North Pacific and negative SLP anomalies over the eastern Asian and Alaska. The SSTA spatial pattern looks like the PDO SSTA pattern shown in Fig. 6a but there are differences in spatial structure in the extratropical Pacific (Fig. 6b) that is consistent with a degree of orthogonality between these two modes (although defined on different quantities). The change of NPGO pattern after 2007 is conspicuous: There is a quadrupole SLP anomaly pattern that is associated with a significant cooling that extends all the way from the Bering Sea, to the northeastern Pacific, and to the central tropical Pacific (Fig. 6d), while the NPGO pattern during this period shows similarities to the PDO pattern. Thus, both the PDO and the NPGO may collaborate in driving the Bering SST anomalies in the later period.

To investigate the time evolution of the PDO and NPGO impact onto the Bering Sea, we regress subsurface ocean temperature averaged over the Bering Sea onto the PDO and NPGO indices using a 241-month running window over the period of 1950-2018 (Fig. 7a & b). The ocean temperature in the Bering Sea indeed exhibits close connection with the PDO since the mid-1970s; a weak connection prior to this period may reflect sparseness of subsurface observations. The correlation first appears in the subsurface layer, then enhances and extends upward with the time, reaching its peak near the surface after 2000. Approximately positive one standard deviation of PDO index corresponds to a maximal 0.35℃ warming in the Bering Sea surface layer. The impact of NPGO, however, on the Bering Sea is significant only during the 1970s-1980s and after 2005. The post-2005 cooling in association with the NPGO positive phase peaks in the subsurface layer rather than in surface. We further calculate the partial correlation coefficients between the Bering temperature and the PDO (NPGO) with the effect of NPGO (PDO) removed (Fig. S1). The spatial patterns of partial correlation analysis shows little change with those in Fig. 7a & b; this corroborates the robustness of the different PDO and NPGO relation to the surface and subsurface ocean temperature in the Bering Sea.

The PDO and NPGO indices become more correlated during the most recent period, as shown by a 241-month running correlation between the two indices (Fig 7c). The PDO and NPGO remain almost zero correlations until the end of 1980s, thereafter they become more and more correlated. In the 21st century, the monthly correlation coefficient reaches to -0.4, or even -0.6 with the seasonal variations being filtered out. The increasing synchronization of the PDO and NPGO mode can be clearly detected even by comparing their time series (Fig. 8). The decadal amplitude of NPGO is almost doubled from the end of 1980s. The strengthening of NPGO coalesces with the PDO to be in an apparent

anti-resonance after 2007 (as the patterns are negatively spatially correlated, this SST patterns reinforce each other).

Yeo et al. (2014) also demonstrated that the Chukchi-Bering climate variability for the post-1999 period is closely related to Pacific basin-scale atmospheric and oceanic circulation patterns, e.g., the North Pacific Oscillation (NPO), the North Pacific Gyre Oscillation (NPGO) as well as the central Pacific El Niño. Indeed, the SBII time series in Fig. 2b exhibits an obvious change in its periodicity. The SBII varied mainly in interannual time scale before 2000, and thereafter in decadal time scale, coinciding with the NPO-NPGO variability in 1999-2010. But it is only until after ~2007 when the NPGO and PDO indices vary out-of-phase that the Arctic sea ice variance exhibits the obvious decadal change along with the enhanced decadal oscillation of SBII. The detailed physical mechanism for the apparent changes in the PDO and NPGO patterns deserves further investigation that is beyond the scope of this paper.

~~To explore the mechanism that is responsible for recent ocean dominant ice variation, we composite the Bering Sea zonal mean (160°200°E mean) temperature anomalies (with PDO removed) based on the SBII high minus low index for the two periods, as shown in Fig. 5 a & b. In the early period, the expansion of spring Bering ice cover corresponds to the significant cooling in the upper ocean extending from sea surface to the subsurface layer at the southern flank of Bering Strait (Fig. 5a). The significant subsurface cooling reappears in recent decade with its maxima centered in 100-300m, but the surface cooling is insignificant (Fig. 5b). This further underlines the ocean role in facilitating the increase of Bering Sea ice area. The 11-year running trends of ocean temperature in the Bering Sea area (160°200°E, 55°65°N mean) are displayed in Fig. 5c. It is as expected that the remarkable cooling trends emerge after ~2007, with the maximum at subsurface layer of ~165m.~~

~~To validate this result, we compared the time series of 3-month running mean temperature at 165m from the ORAs4 data with those from the GODAS and HadEN4 datasets (Fig. 6). All three datasets agree on the abrupt descent of subsurface temperature in recent decade, in spite of the discrepancies in their transition time and amplitude within limits. In particular, the ORAs4 temperature shows the greatest drop of ~0.8℃ in the time of 2007. The HadEN4 data is consistent with the ORAs4 in transition time but in smaller amplitude, while the transition time of GODAS temperature is two-year earlier than the other two datasets.~~

~~What triggered the abrupt drop of temperature in the Bering Sea upper ocean after 2007? Fig. 5d shows the climatological change of temperature and ocean circulation in subsurface Bering Sea at 165m for the prior and post 2007 periods. The recent subsurface cooling in Bering Sea corresponds to an anomalous anticyclone circulation in the Bering Sea. The climatological circulation in Bering Sea is characterized by a cyclonic gyre, composed of a strong western boundary cold current (i.e., East Kamchatka Current) and a weak and warm Alaska stream (figure not shown). This anomalous anticyclone circulation is associated with the dramatic decrease of the warm advection by the Alaska stream, which may lead to the cooling in the Bering Sea. Another possible factor accounting for the Bering Sea cooling is the local wind stress. There is an anomalous high pressure and correspondingly anticyclonic atmosphere circulation over the Bering Sea in recent decade (Fig. 7). The anomalous southwestlies over the northwest of Bering Sea tend to induce the coastal upwelling of colder deep water along the coast, thereby facilitates the cooling in the northern Bering Sea. More detailed diagnostics and analysis are required to ascertain the dynamical processes for the recent subsurface cooling in the Bering Sea.~~

3.4 Distinct effects of PDO and NPGO on the Bering Sea

From the statistical analyses in the section 3.3, the NPGO and PDO changes may be responsible for the recent increase in SBII multi-year variability via their influence on the surface and subsurface ocean temperature in the Bering Sea. Here we investigate the physical linkages between these large-scale climate modes and the Bering Sea. In spite of high resemblance of their SSTA pattern after 2007, the SLP patterns related to the PDO and the NPGO differ greatly (Fig. 6 c & d). This implies distinct oceanic mechanisms in these two modes. The atmospheric thermal forcing is estimated by regressing the turbulent heat flux anomalies onto the PDO and the NPGO indices (Fig. 9). There are hardly any significant PDO-related heat flux anomalies in the Bering Sea region during either period (Fig. 9a & c). The positive phase of NPGO corresponds to the negative anomalies of heat flux along the northwest coast of Bering in the early period (Fig. 9b). In the later period, the NPGO is associated with positive and negative anomalies of heat flux appear in the southern and northern Bering Sea respectively, with the zero correlation line approximately along the climatological spring Bering Sea ice edge (Fig. 9d). Referring to the NPGO-related quadruple SLP pattern (Fig. 6d), the anomalous atmospheric cold advection associated with the anomalous high pressure prevails over the Bering Sea, and is consistent with the drop in atmospheric surface temperature and increased heat loss over the open ocean, and hence

the SST cooling. The sea ice expansion follows the decreasing temperature and insulates the ocean-atmosphere exchange, resulting in the negative anomalies of heat flux over the ice cover. This may partly explain the enhanced Bering Sea surface cooling associated with the NPGO in the later period (Fig. 6d). It should be noted that the NPGO-related high-pressure anomalies over the Bering Sea extends westward to the eastern Siberian, which is quite similar to the SBII-related SLP anomalous structure (Fig. 3d). This underlines the contribution of NPGO atmospheric anomalies in forcing the Bering Sea surface response.

The atmospheric dynamical forcing on the upper ocean circulation is assessed by regression of spring wind stress and Ekman pumping rate anomalies onto the PDO and NPGO indices (Fig. 10). In response to the deepening of Aleutian Low (Fig. 6a & c), positive phase of PDO is associated with an anomalous cyclonic circulation over the north Pacific, without any notable change between the two periods considered. The relevant positive Ekman pumping anomalies mainly reside in the north Pacific open ocean, while the enhanced northeasterly prevails over the entire Bering Sea (Fig. 10a & c). In contrast, the NPGO has hardly any impact on the large-scale circulation. Nevertheless, the scattered significant wind stress anomalies in the later period organize an anomalous anti-cyclonic pattern, hence the negative Ekman pumping rate (downwelling) in the western Bering Sea (Fig. 10d). The vertical velocity induced by surface wind stress curl usually results in the displacement of thermocline or pycnocline, followed by the dynamical adjustment of the subsurface ocean.

The climatological upper ocean circulation in the Bering Sea and the adjacent region is primarily characterized by a cyclonic circulation, primarily composed of warm Alaska stream, cold Kamchatka current, and the Bering slope current (figure not shown). Given the significant wind stress forcing in accordance with PDO, the spring ocean velocity and density anomalies are regressed on the PDO index both in the surface (5m) and subsurface (165m) layer (Fig. 11). The regression is done for the whole period because the PDO exhibits little change between the periods. The large-scale cyclonic wind stress anomalies associated with the PDO positive phase lead to the strengthening of Alaska stream and enhanced northward heat transport along the Bering slope, contributing to the surface warming and density decrease in the Bering Sea (Fig. 11a). In the subsurface layer, however, the wind-driven component abates rapidly with depth. The anomalous heat transport is limited to the boundary current around the southern Bering deep basin (Fig. 11b). Therefore, the Bering Sea warming associated with PDO peaks in the surface layer. The circulation anomalies corresponding to the NPGO is also

investigated, but without any remarkable signal of current and heat transport anomalies (figure not shown).

In consideration of the significant NPGO-related Ekman pumping rate (Fig. 10d) and subsurface cooling (Fig. 7b), the pycnocline displacement and vertical exchange between the mixed layer and subsurface ocean in the Bering Sea deep basin (160-190°E, 50-60°N) is investigated. The climatological vertical profile of temperature (T), salinity (S) and density (Rho) in this region in spring is presented in Fig. 12. The vertical stratification of Bering basin depends on salinity, with the closely matching position of the pycnocline and halocline at about 100-300m depth. In striking contrast to the increase of salinity and density with depth, the temperature profile exhibits a sandwich-like pattern. There is a sharp rising of temperature from ~2.5℃ to ~3.5℃ in 100-300m, then slowly drop down with depth below the permanent pycnocline. It is clear that the cold and fresh water in the mixed layer is superposed over the warm and saline water in the pycnocline. The spring Bering Sea deep-basin hydrographic anomalies associated with positive NPGO for different periods are shown in Fig. 13. In the early period, the NPGO-related changes of water property are confined to the mixed layer. In the later period, the hydrographic anomalies associated with positive NPGO almost doubled in the mixed layer, and the change in the pycnocline can be detected clearly. The colder and saltier water in the surface overlies the less cold and fresher water in the subsurface, corresponding to the density increase (decrease) in the mixed layer (pycnocline).

A NPGO-related atmosphere-ocean-ice mechanism may be depicted as follows: The quadrupole SLP pattern in the recent decade (Fig. 6d) favors the atmospheric cold advection and anticyclonic wind stress curl (Fig. 10d) over the Bering Sea in association with positive phase of NPGO. In response to atmospheric thermal forcing, ocean heat loss enhances in the open water (Fig. 9d), leading to the greater surface cooling. On the other hand, the Bering sea ice cover expands with the cooling condition. Ice expansion is usually followed by surface salinification in the adjacent open water owing to brine-rejection effect. Surface water is getting denser with the anomalous cooling and salinification. Triggered by the anticyclonic wind stress curl over the Bering basin region, anomalous downwelling acts to push the subsurface isopycnals downward, hence the decrease of density and freshening in the pycnocline with the positive NPGO (Fig. 13b). The reverse processes may occur for the negative NPGO phase: atmospheric warm advection leads to less heat loss from ocean and retreat of sea ice cover, thus warming and freshening of surface water. The surface density decreases to a large extent.

The cyclonic wind stress forcing and the subsequent upwelling induce the heaving of subsurface isopycnals, hence increased density and salinification in the pycnocline. The NPGO leads to variations over deeper part of the upper ocean and this can explain a stronger impact on the seasonal cycle, as compared to periods when only the PDO influences the upper ocean of the region.

To further verify the sensitivity of SBII to the NPGO-oriented physical processes in the most recent period, the spring wind stress and Ekman pumping rate anomalies are composited based on the SBII high minus low index years for both periods (Fig. 14). The spring Bering sea ice cover expansion corresponds to the prevailing northerly over the Bering Sea and a large-scale anticyclonic circulation and upwelling in the North Pacific Ocean in the early period (Fig. 14a), which resembles the PDO-related pattern (Fig. 10a). For the later period, there are anomalous anticyclonic wind stress curl over the Bering Sea and downwelling in association with the increased ice extent (Fig. 14b), and this resembles the NPGO-related pattern (Fig. 10d). In addition, the Bering deep-basin water property changes in association with the SBII high minus low index years are presented in Fig. 15. In the early period, the ice expansion corresponds to the surface cooling but little change in the salinity and density (Fig. 15a). In the later period, the ice expansion corresponds to much larger magnitude of surface cooling as well as salinity and density anomalies. The changes can also extend to pycnocline layer with the reverse of the salinity and density anomalies vertically, and they resemble the NPGO-related hydrographic anomalies (Fig. 13b). This corroborates that the recent decadal oscillation of the Bering sea ice is primarily attributed to the NPGO pattern change.

4 Conclusions and discussion

By dissecting spatial-temporal variability of the Arctic sea ice, this study identifies the recent multi-year variability in spring Bering Sea ice extent has been one of the main factors enhancing the seasonality of total Arctic sea ice. ~~investigated t~~The physical mechanism ~~that accounts for~~underlying the decadal change of spring Bering Sea ice extent is explored. The results show that the prominent decadal oscillation of spring Bering Sea ice is triggered by the NPGO pattern change and its synchronization with the PDO. The PDO influences the SST anomalies in the Bering Sea via its effect on the ocean heat advection, which shows little variation during the different periods. The NPGO, on the other hand, shows conspicuous changes in the new century. After 2007, the NPGO is associated with an SLP quadrupole pattern with anomalous anticyclonic wind stress curl over the Bering basin. The subsequent Ekman

pumping rate anomalies induce the vertical undulation of pycnocline, leading to significant water property change in the subsurface layer.

It is worth noting that the decadal oscillation of Bering sea ice extent occurs only in spring season, but not in winter. We then examine the time series of winter (Dec-Feb mean) Bering sea ice extent. The winter Bering sea ice cover remains relative stable until 2014. Thereafter a drastic ice decline occurs in the recent five years (Fig. S2), which is highly consistent with the abnormal atmospheric warming over the Bering Sea (Fig. 5a). The regressions of various physical fields onto the PDO and NPGO are repeated for the winter (Dec-Feb mean) season (Fig. S3 & S4). The SST and SLP anomalies associated with the PDO in winter season (Fig. S3a & c) looks much like those in spring season. The NPGO-related anomalous SST pattern shows little changes in winter, comparing to the pattern in spring. But there is discernable discrepancy of SLP anomalies between the two seasons. The winter NPGO-related SLP anomalies for the prior-2007 period exhibits the typical North Pacific Oscillation (NPO) pattern, with the SLP negative anomalies and positive anomalies to the north and south side of 45 ºN, respectively (Fig. S3b). For the post-2007 period, the NPO-like SLP dipole pattern seems shifted toward southeast. The eastern Siberian is resided by an anomalous polar high pressure. The Bering Sea is located at the nodal line between the northwest positive and southeast negative SLP anomalies (Fig. S3d). As a result, the Bering Sea is prevailed by northeasterly wind without any marked anomaly in wind stress curl and Ekman pumping rate (Fig. S4d), thus no subsurface response. Therefore, the winter Bering Sea ice varies along with the surface air temperature, but with no decadal oscillation. This further demonstrates that the subsurface ocean response to the NPGO-related surface atmospheric forcing is a key process for the Bering Sea ice decadal change in spring.

A natural question is why the NPGO pattern exhibits such a remarkable change in spring and its evolution coincides with PDO after 2007. As the second mode of sea surface height anomalies in northeast Pacific, the NPGO mode is driven either by local stochastic atmospheric processes (represented of North Pacific Oscillation) or by tropical ocean forcing (mostly related to central-Pacific El-Niño event) remotely (Di Lorenzo et al. 2008; 2010). Therefore, the NPGO changes may be traced to the changes in the background atmospheric circulation and in the tropical Pacific thermal state. The Pacific atmospheric circulation is predominated by the Aleutian Low (AL) variability and/or its coherence with the subtropical Hawaii High, which can be largely represented by a North Pacific Index (NPI, Hurrell et al., 2019). The low-frequency (20-year low-pass filtered) variability of spring

(March-May mean) NPI shifts from negative phase (deepening of Aleutian Low) since 1979 to positive phase in around 2007. Correspondingly, the climatological spring SLP pattern in the post-2007 shows a weak eastward shift of Aleutian Low relative to the 1979-2007 period (Fig. S5). This may contribute to the shift of NPGO-related SLP anomalies, from dipole to quadrupole pattern. The SST pattern change in NPGO mode, on the other hand, may be more releated to the tropical variations. Numerous studies have asserted the increasing ratio of central Pacific warming to the canonical eastern Pacific warming since the late twentieth century (Lee and McPhaden 2010; Yu et al. 2010; Liu et al. 2017; Freund et al. 2019). The transition of tropical Pacific thermal state may trigger the decadal changes of NPGO. We further examine the NPGO definition and repeat the same SSH EOF analysis in the Northeast Pacific (180 ºW-110 ºW, 25 ºN-62 ºN) as Di Lorenzo et al. (2008). The running correlation of Lorenzo's NPGO index and the SSH EOF PC1 and PC2 shows an obvious decadal change in the late 1990s, after which the NPGO is much more significantly correlated with the EOF PC1 than PC2 (Fig. S6). Further SSH EOF analysis during two separate period (1979-1998 vs. 1999-2017) confirms that spatial pattern of SSH second EOF mode in the later period is totally different from that in the early period, as well as from canonical NPGO pattern (Fig. S7). This may related to the change in the NPGO pattern and its synchronism with PDO. More detailed analysis is needed to explore the connection of tropical Pacific thermal state change with the northeast Pacific dynamical response.

~~the amplifying seasonal cycle of total Arctic SIE in recent decade. The key point accounting for the increased amplitude of seasonal cycle lies in the Bering Sea, where the sea ice cover expands due to the significant subsurface cooling in recent decade. This, in great contrast to the continuous surface warming in the pan-Arctic region, may shed light on the future Arctic climate change.~~

Woodgate et al. (2010) reported the increasing oceanic heat flux over the Bering Strait since the early 2000s, and proposed that this Bering Strait inflow may act as a conduit for oceanic heat into the Arctic and contribute to the unprecedented seasonal Arctic sea-ice loss in 2007. Echoing to this increasing heat flux into the Arctic Ocean, the Bering Sea is reported to be the only substantial non-coastal area with lengthening sea ice seasons within the Pan-Arctic region (Parkinson, 2014). However, the Bering Sea ice cover in these five years experiences a cascading decline, particularly in 2018 and 2019 years. This abrupt change may be attributed to the collective effect of Arctic climate change and the recent Pacific decadal variability, i.e., the Arctic surface warming and the local subsurface change. The Bering Sea change, in turn, could feedback to the central Arctic Ocean by

modulating Bering Strait throughflow strength as well as the heat and freshwater transport through the strait. Therefore, further study is necessary to determine the complicated and interweaving physical processes that may lead to the recent Arctic climate change. In the background of global warming and polar amplification, the total Arctic ice volume and thickness decrease persistently. It is conceivable that the future change of Arctic sea ice extent is more sensitive to the complicated air-sea coupling processes. Here we have contributed to further understand the Bering Sea thermal state and dynamical processes, as well as its connection to the North Pacific climate change. Further work is required in order to answer questions like whether this tendency of amplifying seasonal cycle of Arctic sea ice cover will be sustained or not and whether it will lead to the nonlinear instability of the Arctic climate system.

~~Our result is generally consistent with these previous studies: The increasing oceanic heat flux over the strait may lead to anomalous warming in the central Arctic Ocean and cooling in the Bering Sea, therefore the seasonal contrast of sea ice variability in the Pacific sector and the lengthening sea ice season in the Bering Sea. By the preliminary analysis, we go further to propose that the decadal change of local oceanic and atmospheric circulation change, i.e., the anomalous oceanic temperature advection and/or the coastal upwelling may account for the abrupt subsurface cooling in the Bering Sea after 2007.~~

~~In addition to local dynamical processes, previous studies also demonstrated that the Chukchi Bering climate variability for the post 1999 period is closely related to Pacific basin scale atmospheric and oceanic circulation patterns, e.g., the North Pacific Oscillation (NPO), the North Pacific Gyre Oscillation (NPGO) as well as the central Pacific El Nino (Yeo et al., 2014). Indeed, the SBII time series in Fig. 1d exhibits an obvious change in its period. The SBII varied mainly in the interannual time scale before 2000, and after that in decadal time scale, coinciding with the NPO-NPGO couple mode in 1999-2010. In this sense, the abrupt Arctic sea ice cover change may also connect to the Pacific climate regime shift. Therefore, further study is necessary to undermine the leading player in the recent Arctic climate change. In order to answer the questions like whether this tendency of amplifying seasonal cycle of Arctic sea ice cover will sustained or not and whether it will lead to the nonlinear instability of the Arctic climate system, we should improve our understanding on the Bering Sea thermal state and dynamical processes as well as its connection to the North Pacific climate mode.~~

Data availability. NSIDC monthly sea ice satellite product can be downloaded via http://nsidc.org/data/nsidc-0051.html. ERA-interim reanalysis dataset is provided by ECMWF on their

website https://apps.ecmwf.int/datasets/data/interim-full-moda/levtype=sfc/. ORA-S4 ocean reanalysis dataset is supplied by https://climatedataguide.ucar.edu/climate-data/oras4-ecmwf-ocean-reanalysis-and-derived-ocean-heat-content. OAflux surface turbulent heat flux data is downloaded via ftp://ftp.whoi.edu/pub/science/oaflux/data_v3. GODAS reanalysis, HadISST and HadEN4 subsurface ocean data are available from Asia-Pacific data-research center of the IPRC via http://apdrc.soest.hawaii.edu/data/data.php.

Author contribution. X.-Y. Yang designed this study and analyzed data. All authors contributed to the interpretation of the results. X.-Y. Yang wrote the manuscript with input from all authors.

Competing interests. The authors declare that they have no conflict of interests.

Acknowledgments

We thank ECMWF for providing the reanalysis datasets of ERAinterim and ORA-s4, and NSIDC for providing the sea ice concentration dataset. We greatly appreciated John E. Walsh and the other anonymous reviewer for their insightful suggestions and generous help in improving the quality of this study.

X.-Y. Yang is supported by the Natural Science Foundation of China (Grant 41576178). G. Wang is supported by the Natural Science Foundation of China (91428206, 91528304), the National Program on Global Change and Air-Sea Interaction (GASIIPOVAI-04) and Program ~~Of~~of Shanghai Academic Leader (17XD1400600).

References

Armour, K. C., Eisenmann, I., Blanchard-Wrigglesworth, E., McCusker, K. E., and Bitz, C. M.: The reversibility of sea ice loss in a state-of-the-art climate model, Geophys. Res. Lett., 38, L16705, doi: 10.1029/2011GL048739, 2011.

Balmaseda, M. A., Mogensen, K., and Weaver, A. T.: Evaluation of the ECMWF ocean reanalysis system ORAS4, Q. J. Roy. Meteor. Soc., 139, 1132-1161, doi: 10.1002/qj.2063, 2012.

Bathiany, S., Notz, D., Mauritsen, T., Raedel, G., and Brovkin, V.: On the potential for abrupt Arctic winter sea ice loss, J. Clim., 29, 2703-2719, doi: 10.1175/JCLI-D-15-0466.1, 2016a.

Bathiany, S., Bolt, B. van der, Williamson, M. S., Lenton, T. M., Scheffer, M., Nes, E. van, and Notz, D.: Trends in sea-ice variability on the way to an ice-free Arctic, The Cryosphere Discussions, doi: 10.5194/tc-2015-209, 2016b.

Cavalieri, D. J., Parkinson, C. L., Gloersen, P., and Zwally, H. J.: Sea ice concentrations from *Nimbus*-7 SMMR and DMSP SSM/I-SSMIS passive microwave data, version 1 [dataset], National Snow and Ice Data Center, accessed March 2014, Available online at http://nsidc.org/data/nsidc-0051.html, 2013.

Ceballos, L. I., Di Lorenzo, E., Hoyos, C. D., Schneider, N., and Taguchi B.: North Pacific Gyre Oscillation synchronizes climate fluctuations in the eastern and western boundary systems, J. Clim., 22, 5163-5174, 2009.

Close, S., Houssais, M. –N., and Herbaut, C.: Regional dependence in the timing of onset of rapid decline in Arctic sea ice concentration, J. Geophys. Res., 120(12), 8077-8098, doi: 10.1002/2015JC011187, 2015.

Cohen, J., Screen, J. A., Furtado, J. C., Barlow, M., Whittleston, D., Coumou, D., Francis, J., Dethloff, K., Entekhabi, D., Overland, J., and Jones, J.: Recent Arctic amplification and extreme mid-latitude weather, Nature Geosci., 7, 627-637, doi: 10.1038/NGEO2234, 2014.

Comiso, J. C., Parkinson, C. L., Gersten, R., and Stock, L.: Accelerated decline in the Arctic sea ice cover, Geophys. Res. Lett., 35, L01703, doi:10.1029/2007GL031972, 2008.

Comiso, J. C.: Large decadal decline of the Arctic multiyear ice cover, J. Clim., 25, 1176-1193, 2012.

Dee, D. P., and coauthors: The ERA-Interim reanalysis: Configuration and performance of the data assimilation system, *Q. J. Roy. Meteor. Soc.*, 137, 553-597, doi: 10.1002/qj.828, 2011.

Di Lorenzo, E., and coauthors: North Pacific Gyre Oscillation links ocean climate and ecosystem change. Geophys. Res. Lett., 35, L08607, doi: 10.1029/2007GL032838, 2008.

Di Lorenzo, E., and coauthors: Central Pacific El Niño and decadal climate change in the North Pacific Ocean. Nat. Geosci., 3, 762-765, doi: 10.1038/NGEO0984, 2010.

Di Lorenzo, E., and coauthors: Synthesis of Pacific ocean climate and ecosystem dynamics, Oceanogr., 26(4), 68-81, 2013.

Duarte, C. M., Lenton, T. M., Wadhams, P., and Wassmann, P.: Abrupt climate change in the Arctic, Nature Climate Change, 2, 60-62, 2012.

Eisenman, I., and Wettlaufer, J. S.: Nonlinear threshold behavior during the loss of Arctic sea ice, PNAS, 106(1), 28-32, doi: 10.1073/pnas.0806887106, 2009.

~~England, M. H., and coauthors: Recent intensification of wind-driven circulation in the Pacific and the ongoing warming hiatus, Nature Climate Change, 4, 222-227, doi: 10.1038/ NCLIMATE2106, 2014.~~

Freund, M. B., Henley, B. J., Karoly, D. J., McGregor, H. V., Abram, N. J., and Dommenget, D.: Higher frequency of central Pacific El Niño events in recent decades relative to past centuries, Nat. Geosci., 12, 450-455, 2019.

Hurrell, J., and NCAR staff: The climate data guide: North Pacific (NP) index by Trenberth and Hurrell; monthly and winter, retrieved from https://climatedataguide.ucar.edu/climate-data/north-pacific-np-index-trenberth-and-hurrell-monthly-and- winter, 2019.

Lee, T., and McPhaden, M. J.: Increasing intensity of El Niño in the central-equatorial Pacific, Geophys. Res. Lett., 37, L14603, 2010.

Lenton, T. M., Held, H., Kriegler, E., Hall, J. W., Lucht, W., Rahmstorf, S., and Schellnhuber, H. J.: Tipping elements in the Earth's climate system, PNAS, 105(6), 1786-1793, doi: 10.1073/pnas.0705414105, 2008.

Lindsay, R. W., and Zhang, J.: The thinning of Arctic sea ice, 1988-2003: Have we passed a tipping point? J. Clim., 18, 4879-4894, 2005.

Liu, Y., and coauthors: Recent enhancement of central Pacific El Niño variability relative to last eight centuries, Nat. Commun., 8, 15386, 2017.

Livina, V. N., & Lenton, T. M.: A recent tipping point in the Arctic sea-ice cover: abrupt and persistent increase in the seasonal cycle since 2007, The Cryosphere, 7, 275-286, doi: 105194/tc-7-275-2013, 2013.

Mantua, N. J., Hare, S. R., Zhang, J., Wallace, J. M., and Francis, R. C.: A Pacific interdecadal climate oscillation with impacts on salmon production, Bull. Amer. Meteor. Soc., 78, 1069-1079, 1997.

Massonnet, F., Vancoppenolle, M., Goosse, H., Docquier, D., Fichefet, T., and Blanchard-Wrigglesworth, E.: Arctic sea-ice change tied to its mean state through thermodynamic processes, Nat. Clim. Change, 8, 599-603, 2018.

Miller, A. J., Chai, F., Chiba, S., Moisan, J. R., and Neilson D. J.: Decadal-scale climate and ecosystem interactions in the North Pacific Ocean, J. Oceanogr., 60, 163-188, 2004.

Newman, M., Compo, G. P., and Alexander, M. A.: ENSO-forced variability of the Pacific Decadal Oscillation, J. Clim., 16(23), 3853-3857, 2003.

Newman, M., and coauthors: The Pacific Decadal Oscillation, revisited, J. Clim., 29, 4399-4427, 2016.

Onarheim, I. H., Eldevik, T., Smedsrud, L. H., and Stroeve, J. C.: Seasonal and regional manifestation of Arctic sea ice loss, J. Clim., 31, 4917-4932, 2018.

Parkinson, C. L.: Spatially mapped reductions in the length of the Arctic sea ice season, Geophys. Res. Lett., 41, 4316-4322, doi: 10.1002/2014GL060434, 2014.

Pinker, R. T., Niu, X., and Ma, Y.: Solar heating of the Arctic Ocean in the context of ice-albedo feedback, J. Geophys. Res.: Oceans, 119, 8395-8409, doi: 10.1002/ 2014JC010232, 2014.

~~Santer, B. D., Wigley, T. M. L., Boyle, J. S., Gaffen, D. J., Hnilo, J. J., Nychka, D., Parker, D. E., and Taylor, K. E.: Statistical significance of trends and trend differences in layer-average atmospheric temperature time series, J. Geophys. Res., 105(D6), 7337-7356, 2000.~~

Schneider, N., and Cornuelle, B. D.: The forcing of the Pacific Decadal Oscillation, J. Clim., 18, 4355-4373, 2005

Screen, J. A., and Simmonds, I.: The central role of diminishing sea ice in recent Arctic temperature amplification, Nature, 464, 1334-1337, doi: 10.1038/nature09051, 2010.

Serreze, M. C., Barrett, A. P., Stroeve, J. C., Kindig, D. N., and Holland, M. M.: The emergence of surface-based Arctic amplification, The Cryosphere, 3, 11-19, 2009.

Serreze, M. C.: Rethinking the sea-ice tipping point, Nature Climate Change, 471, 47-48, 2011.

Stroeve, J. C., Serreze, M. C., Holland, M. M., Kay, J. E., Malanik, J., and Barrett, A. P.: The Arctic's rapidly shrinking sea ice cover: a research synthesis, Climate Change, 110, 1005-1027, doi: 10.1007/s10584-011-0101-1, 2012.

Sydeman, W. J., Santora, J. A., Thompson, S. A., Marinovic, B., and Di Lorenzo, E.: Increasing variance in North Pacific climate relates to unprecedented ecosystem variability off California, Glob. Chang. Bio., 19, 1662-1675, doi: 10.1111/ gcb.12165, 2013.

Tietsche, S., Notz, D., Jungclaus, J. H., and Marotzke, J.: Recovery mechanism of Arctic summer sea ice, Geophys. Res. Lett., 38, L02707, doi: 10.1029/2010GL045698, 2011.

~~Trenberth, K. E., and Fasullo, J. T.: An apparent hiatus in global warming? Earth's Future, 1, 19-32, doi: 10.1002/2013EF000165, 2013.~~

Woodgate, R. A., Weingartner, T., and Lindsay, R.: The 2007 Bering Strait oceanic heat flux and anomalous Arctic sea-ice retreat. Geophys. Res. Lett., 37, L01602, doi: 10.1029/2009GL041621, 2010.

Yeo, S.-R., Kim, K.-Y., Yeh, S.-W., Kim, B.-M., Shim, T., and Jhun, J.-G.: Recent climate variation in the Bering and Chukchi Seas and its linkages to large-scale circulation in the Pacific. Climate Dynamics, 42, 2423-2437, doi: 10.1007/s00382-013-2042-z, 2014.

Yi, D. L., Zhang, L., and Wu, L.: On the mechanisms of decadal variability of the North Pacific Gyre Oscillation over the 20th century, J. Geophys. Res. Oceans, 120, 6114-6129, doi: 10.1002/2014JC010660, 2015.

Yu, J.-Y., Kao, H. -Y., Lee, T., and Kim, S. T.: Subsurface ocean temperature indices for central-Pacific and eastern Pacific types of El Niño and La Nina events, Theor. Appl. Climatol., 103, 337-344, 2010.

Yu, L., X. Jin, and Weller R.: Multidecade global flux datasets from the objectively analyzed air‐sea fluxes (OAFlux) project: Latent and sensible heat fluxes, ocean evaporation, and related surface meteorological variables, OAFlux Project Tech. Rep. OA‐2008‐01, 64 pp, 2008.

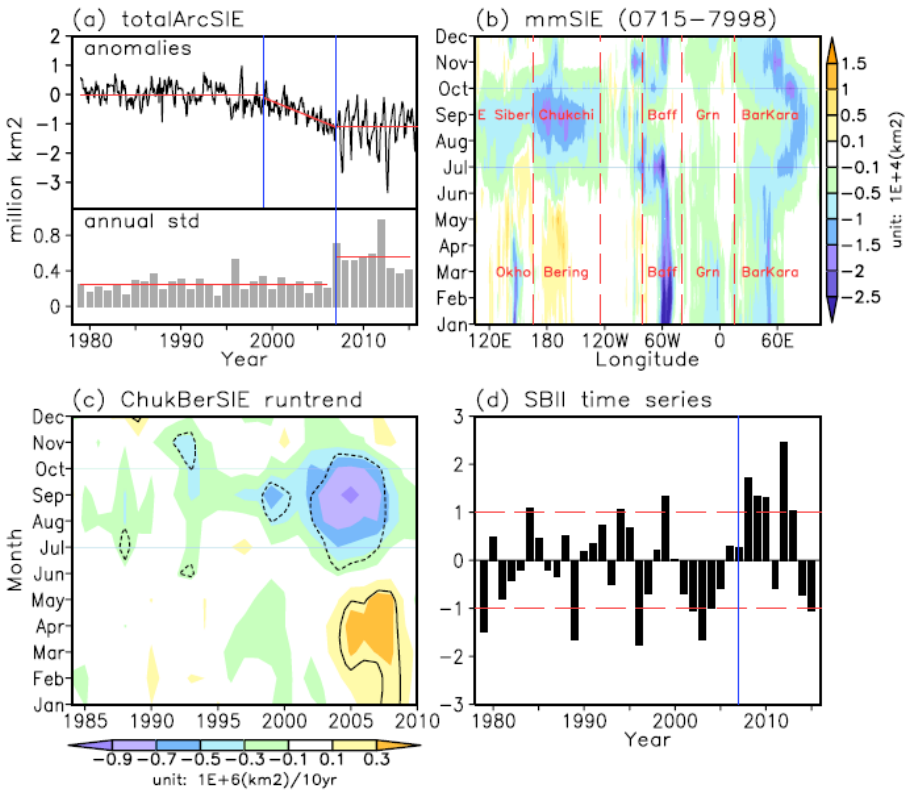

Figure 1: (a) Time series of total Arctic sea ice extent anomalies (upper panel) and annual standard deviation (lower panel) during the period of 1979-2015. Red lines denote the mean values and the linear trend slope for different period. Vertical blue lines indicate the critical years of 1999 and 2007 for the abrupt change of Arctic sea ice cover. (b) Seasonality of sea ice extent climatologic change (2007-2015 mean minus 1979-1998 mean) for each longitude (the red dashed lines roughly demarcate the different sectors of the Arctic marginal seas). (c) Decadal running trends of the Chukchi-Bering sea ice extent for each month. Trends are centered on the indicated year (e.g. the trend at 1985 is based on data from 1980 to 1990). Solid (dashed) lines encircle the positive (negative) trends that exceed the 95% confidence level. (d) Time series of normalized spring (March-May mean) Bering sea ice extent (SBII). Red dashed lines indicate the threshold of ±1 standard deviation for selecting the composite years. Vertical blue line indicates the critical year of 2007.

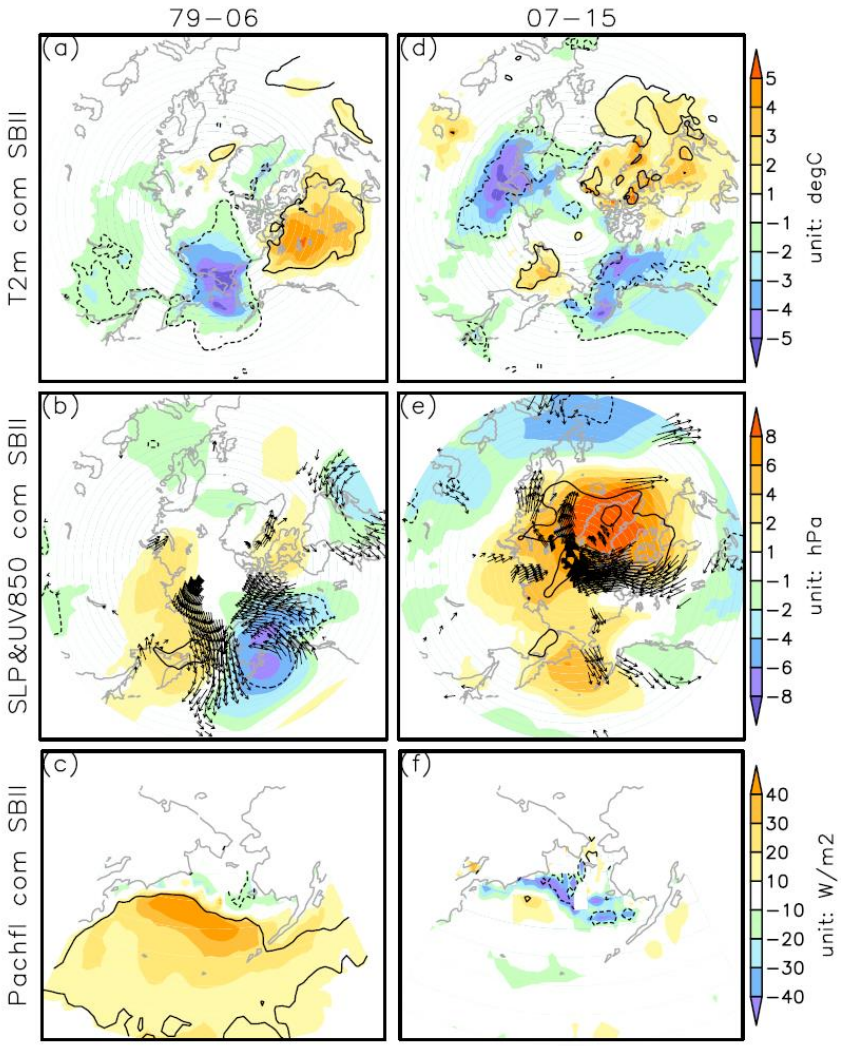

Figure 2. Composites of (a)&(d) 2-metre air temperature anomalies; (b)&(e) sea level pressure (color shading) and 850hPa wind (vectors) anomalies; and (c)&(f) North Pacific turbulent surface heat flux (sensible plus latent heat) anomalies based on SBII high minus low index during the prior 2007 period (left panels) and the post-2007 period. Solid (dashed) lines enclose the positive (negative) values that are significant at the 95% confidence level. For 850hPa wind vectors, only the zonal or meridional wind anomalies that significant at 95% confidence level are displayed.

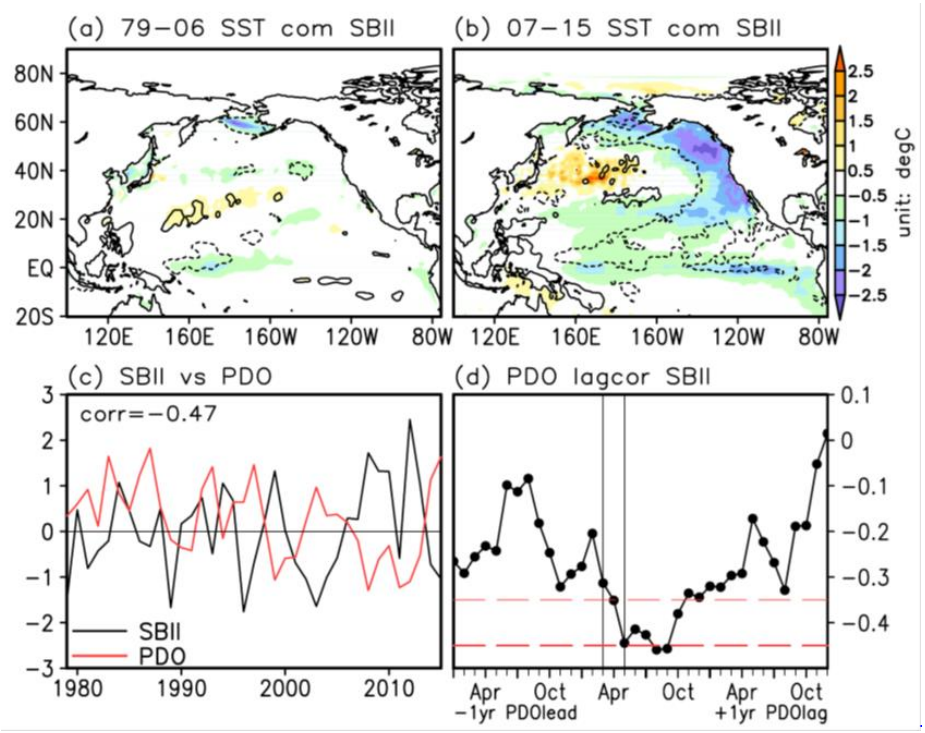

Figure 3. (a) Composite of spring (March-May mean) sea surface temperature anomalies based on SBII during the period of 1979-2006. Solid (dashed) lines enclose the positive (negative) values that are significant at the 95% confidence level. (b) Same as (a), but composite during the period of 2007-2015. (c) Time series of SBII (black) and annual mean PDO index (red). (d) Lead-lag correlation coefficients between the monthly PDO index and SBII. Thin (thick) dashed red lines indicate the 95% (99%) confidence level. Two solid black lines designate the months of March-May, when PDO correlates SBII with zero time lag.

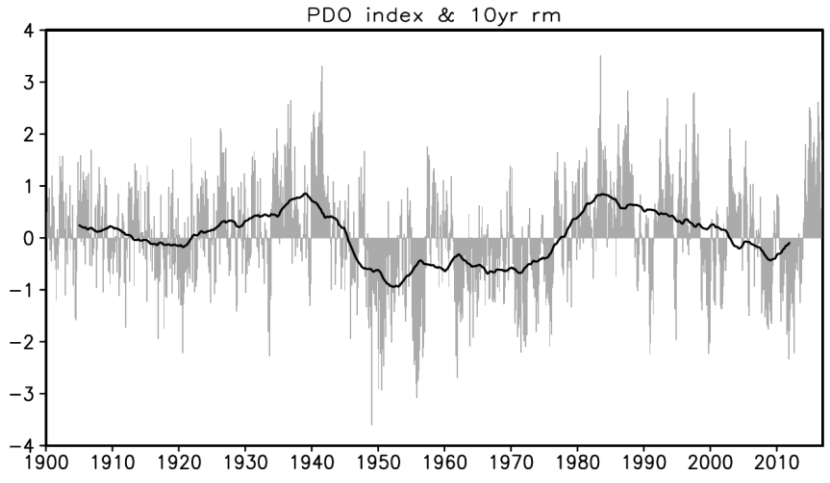

Figure 4. Monthly PDO index (gray bars), superposing its decadal component (120-month running mean, thick black line)

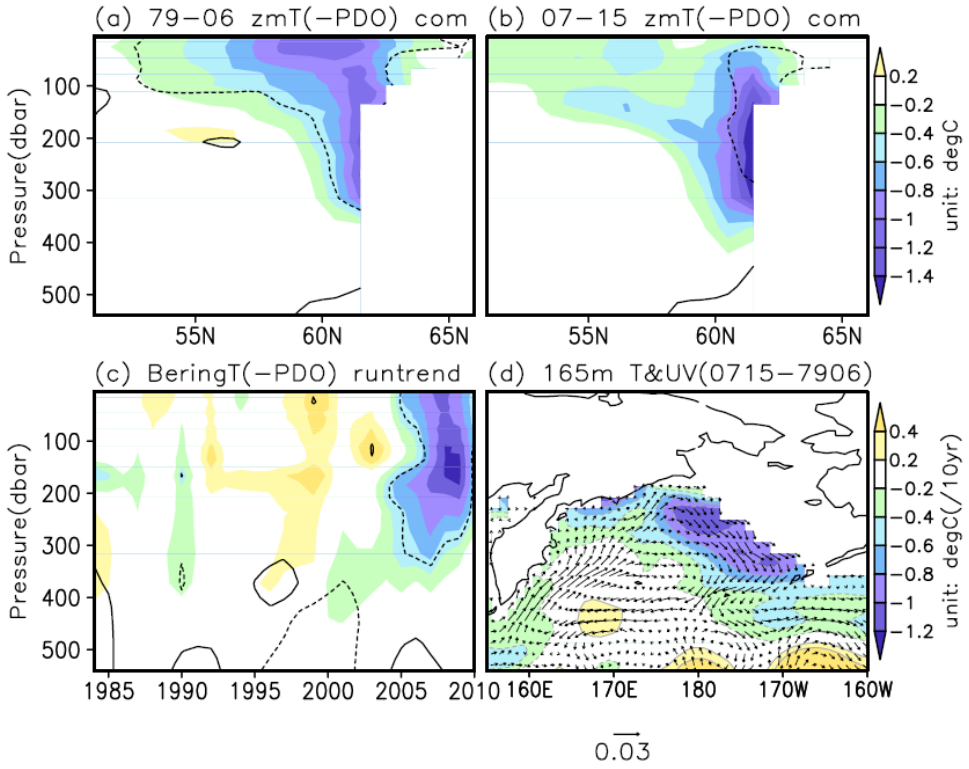

Figure 5. (a) 1979-2006 composites of spring (March-May mean) zonal-mean temperature anomalies (with the PDO-congruent part subtracted from the original data) based on SBII. Solid (dashed) lines enclose the positive (negative) values that are significant at the 95% confidence level. (b) Same as (a), but composites for the period of 2007-2015. (c) 11-year running trends of spring Bering Sea temperature (with the PDO-congruent part subtracted from the original data). Solid (dashed) lines enclose the positive (negative) trends that are significant at the 95% confidence level. (d) Decadal change of temperature (color shading) and horizontal velocity at 165m level with the 2007-2015 mean minus 1979-2006 mean. (c) and (d) share the same color bar with different units, i.e., degC/10yr for (c) and degC for (d).

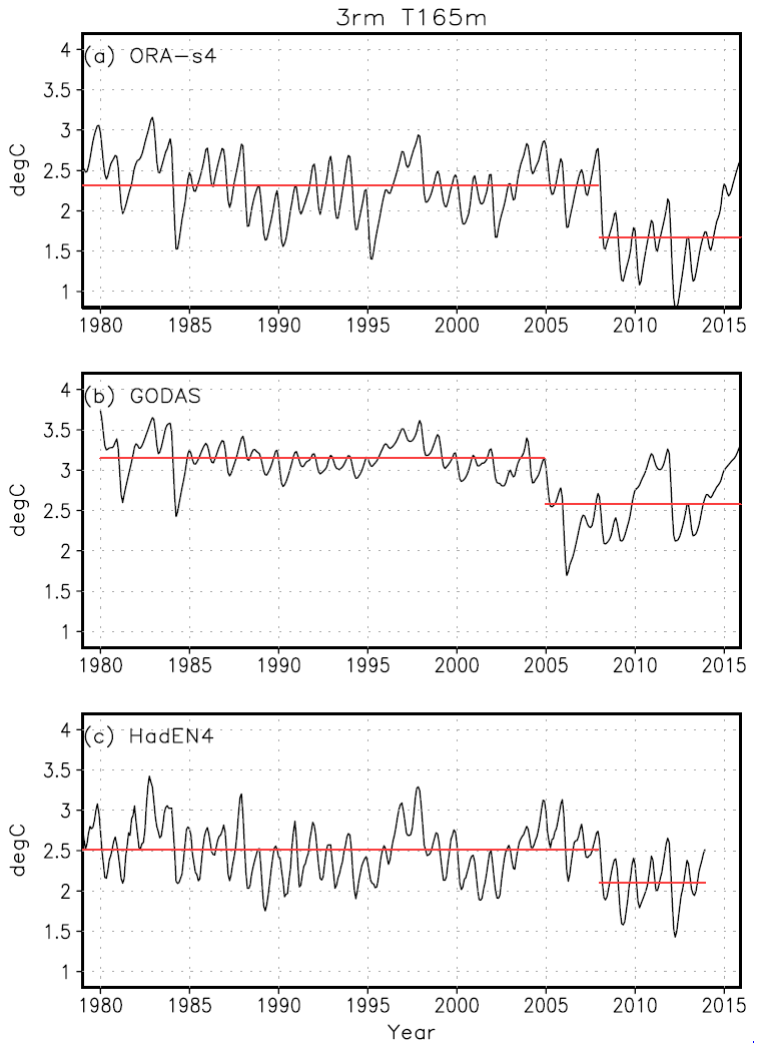

Figure 6. (a) ORA-s4 time series of 3-month running mean subsurface temperature at about 165m depth. The red lines indicate the means for the period of prior- and post- 2007. (b) Same as (a), but for the GODAS dataset. The red lines indicate the means for the period of prior- and post- 2005. (c) Same as (a), but for the HadEN4 dataset.

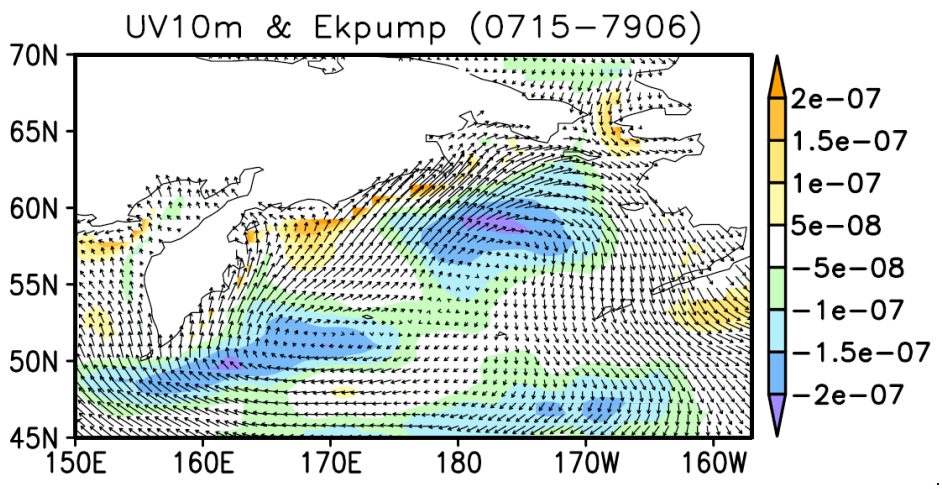

Figure 7. Decadal change of Ekman pumping rate (color shading) and 10m U, V wind (vectors) with the 2007-2015 mean minus 1979-2006 mean.

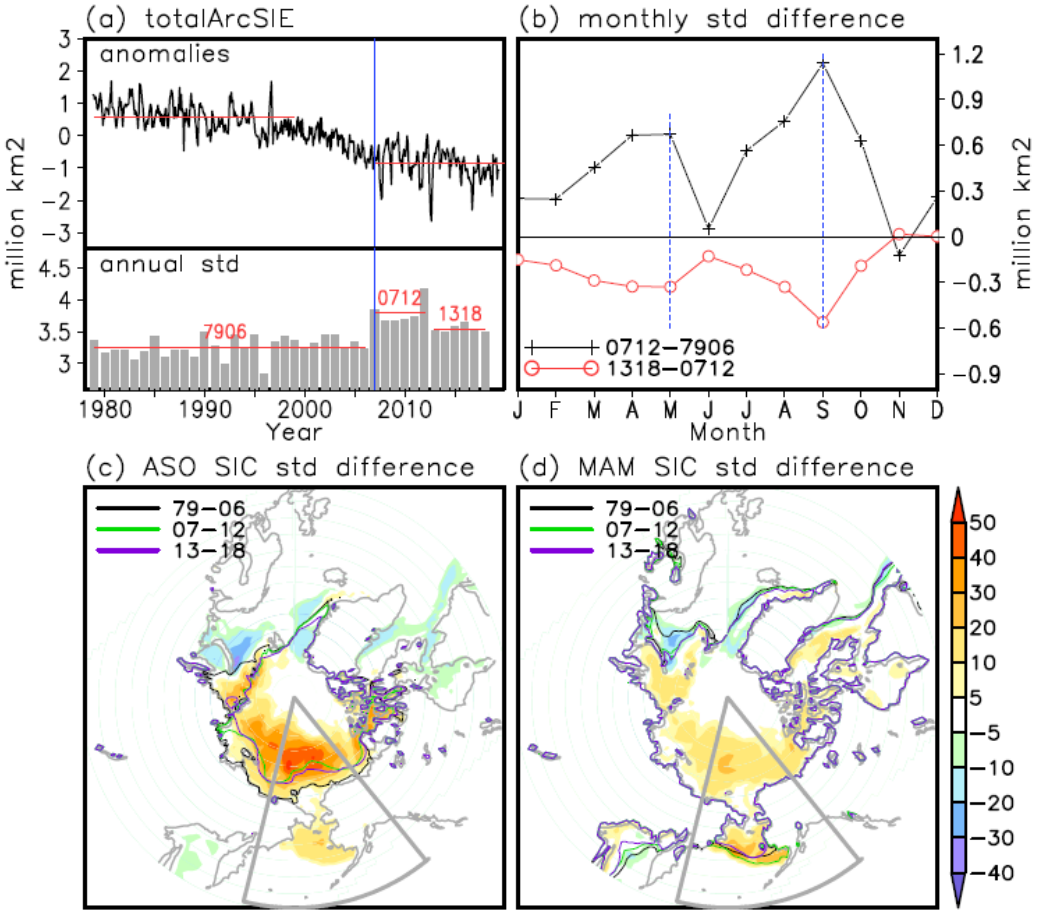

Figure 1. (a) monthly total Arctic sea ice extent (totalArcSIE) anomalies (upper panel) and annual standard deviation (lower panel) during the period of 1978-2019. Red lines denote the mean values for different periods. Vertical blue line indicates the year of 2007. (b) differences of multi-year averaged standard deviations (std) for the different calendar months for the three periods designated in (a) lower panel. Black line denotes the std values of 2007-2012 mean minus 1979-2006 mean. Red line denotes the std values of 2013-2018 mean minus 2007-2012 mean. Blue dashed lines are the two peak months, September (thick) and May (thin). (c) Sum of absolute differences in the August-October mean sea ice concentration (SIC) multi-year averaged standard deviation between the three periods (i.e., the black line peak values minus the red line peak values in (b)). Solid contours marks the climatological sea ice edges (SIC=15%) for three periods. The Pacific sector (Chukchi-Bering) is delimited by the gray fan-shaped frame. (d) Same as (c), but for March-May mean.

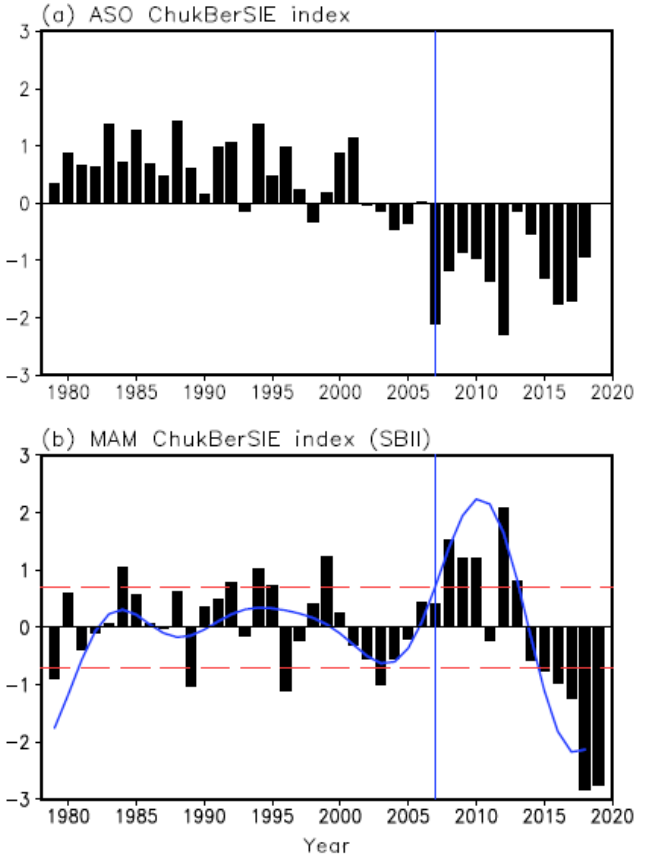

Figure 2. (a) Normalized summer (August-October mean) ChukBerSIE index. (b) Normalized spring (March-May mean) ChukBerSIE index (SBII, black bars), superposed by its decadal component (blue lines). Red dashed lines mark the threshold of ±0.7 standard deviation for selecting the composite years. Vertical blue line indicates the critical year of 2007.

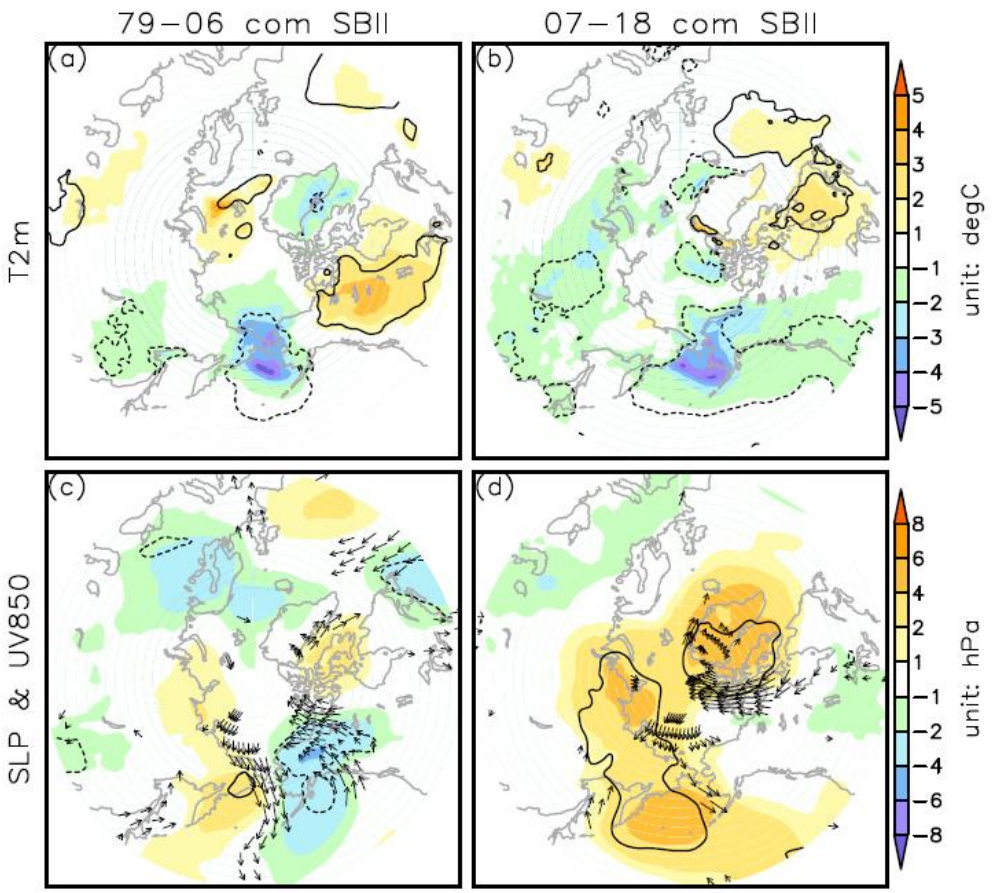

Figure 3. Composites of March-April-May (a)&(b) 2-metre air temperature anomalies; (c)&(d) sea level pressure (color shading) and 850hPa wind (vectors) anomalies based on the SBII high minus low index during the prior-2007 period (left panels) and the post-2007 period (right panels). Solid (dashed) lines enclose the positive (negative) values that are significant at the 95% confidence level. For 850hPa wind vectors, only the meridional wind anomalies that significant at 95% confidence level are presented.

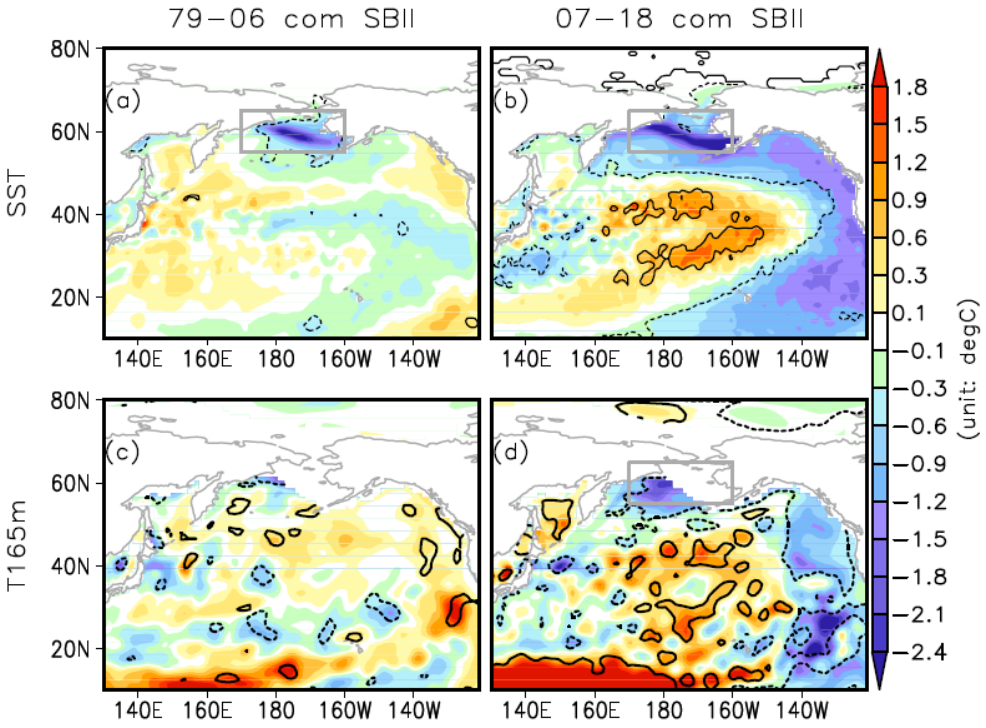

Figure 4. Composites of March-April-May (a)&(b) sea surface temperature anomalies; (c)&(d) subsurface (165m) water temperature anomalies based on the SBII high minus low index during the prior-2007 period (left panels) and the post-2007 period (right panels). Gray rectangle defines the area of Bering Sea (170-200E, 55-65N). Solid (dashed) lines enclose the positive (negative) values that are significant at the 95% confidence level.

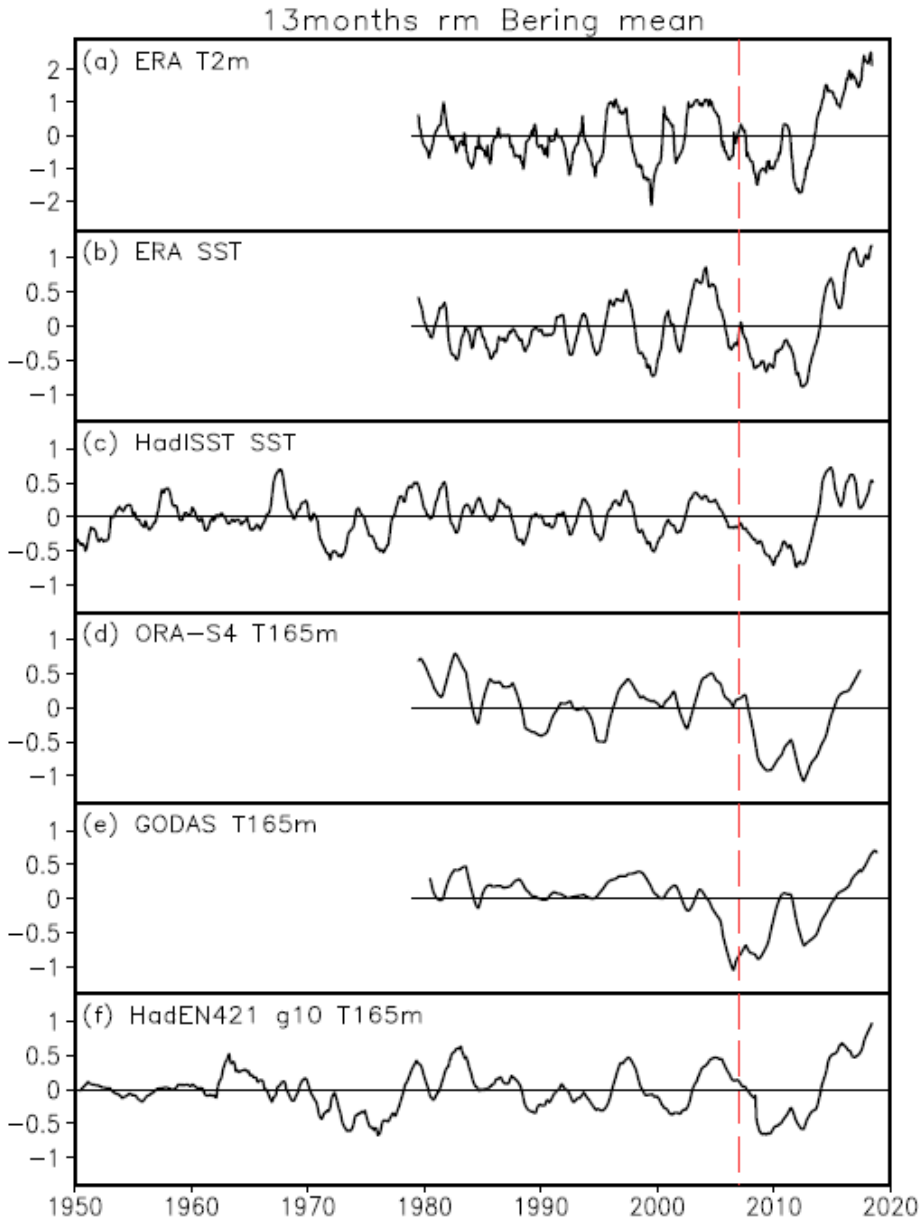

Figure 5. Time series of Bering-mean temperature anomalies from various datasets. (a) ERAinterim 2-metre air temperature; (b) ERAinterim sea surface temperature; (c) HadISST1 sea surface temperature (with the global mean SST subtracted from the original data); (d), (e) & (f) subsurface (165m) temperature from ORA-S4, GODAS and HadEN4.2.1 g10 datasets. All data is low-pass filtered by 13 months running mean. Dashed red line marks the critical year of 2007.

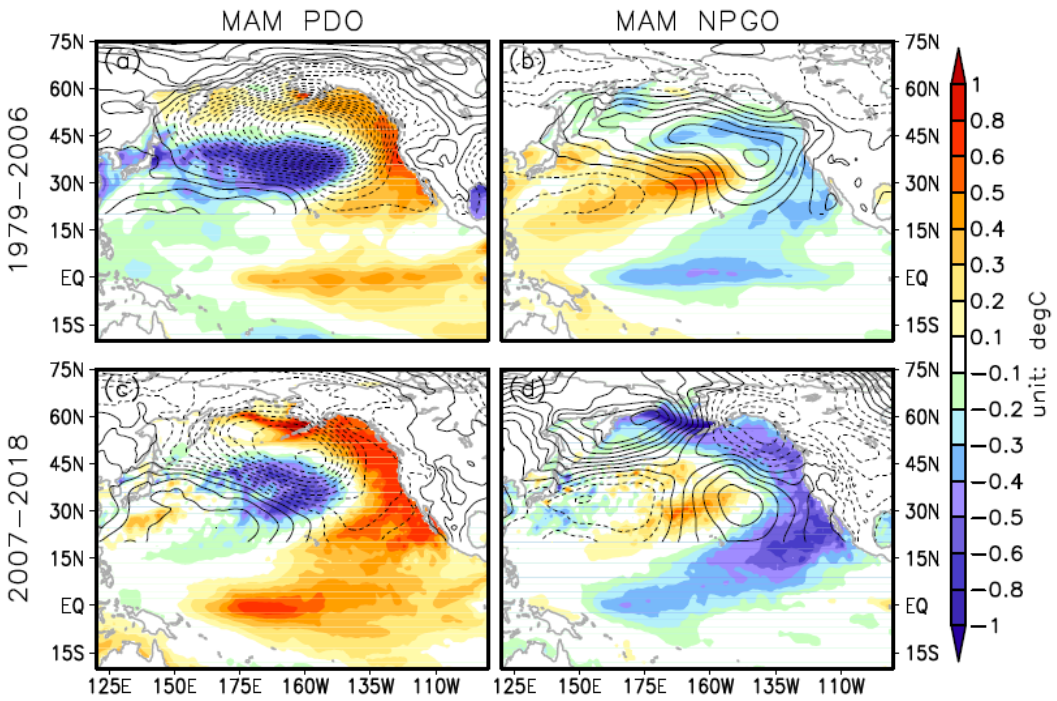

Figure 6. (a) Regression of March-May mean sea surface temperature anomalies (color shading) and sea level pressure anomalies (contour) on the PDO index during the period of 1979-2006. The solid and dashed contours indicate the positive and negative anomalies of SLP. The contour interval is 0.2hPa. (b) Same as (a), but regression on the NPGO index. (c) & (d), same as (a) & (b), but during the period of 2007-2018.

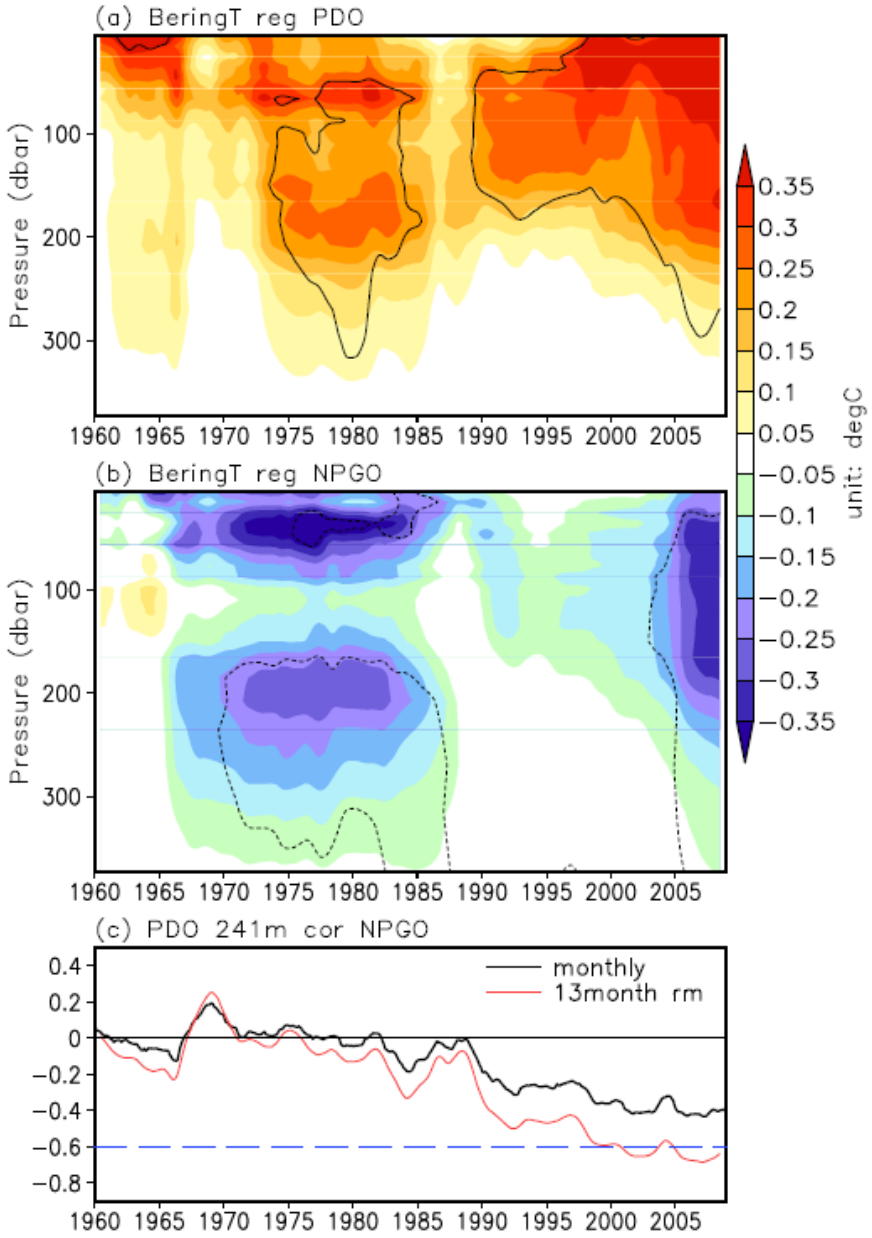

Figure 7. 241-month running regression of the HadEN4 subsurface Bering sea temperature anomalies on the PDO index (a) and the NPGO index (b). All the data are preprocessed by 13 months low-pass filter. Solid (dashed) lines enclose the positive (negative) regression coefficients that are significant at the 95% confidence level. (c) 241-month running correlation between the PDO and NPGO indices. Black (red) lines indicate the original monthly (13 months low-pass filtered) correlation.

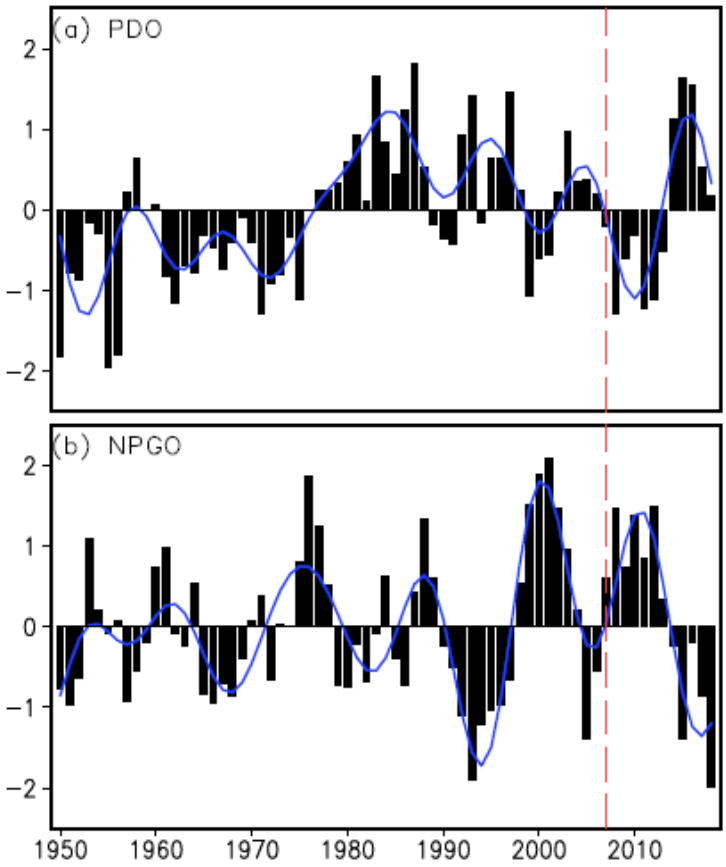

Figure 8. (a) Time series of the annual mean PDO index (black bar) superposed by its decadal component (blue line) during the period of 1950-2018. The red dashed line indicates the critical year of 2007. (b) Same as (a), but the NPGO index.

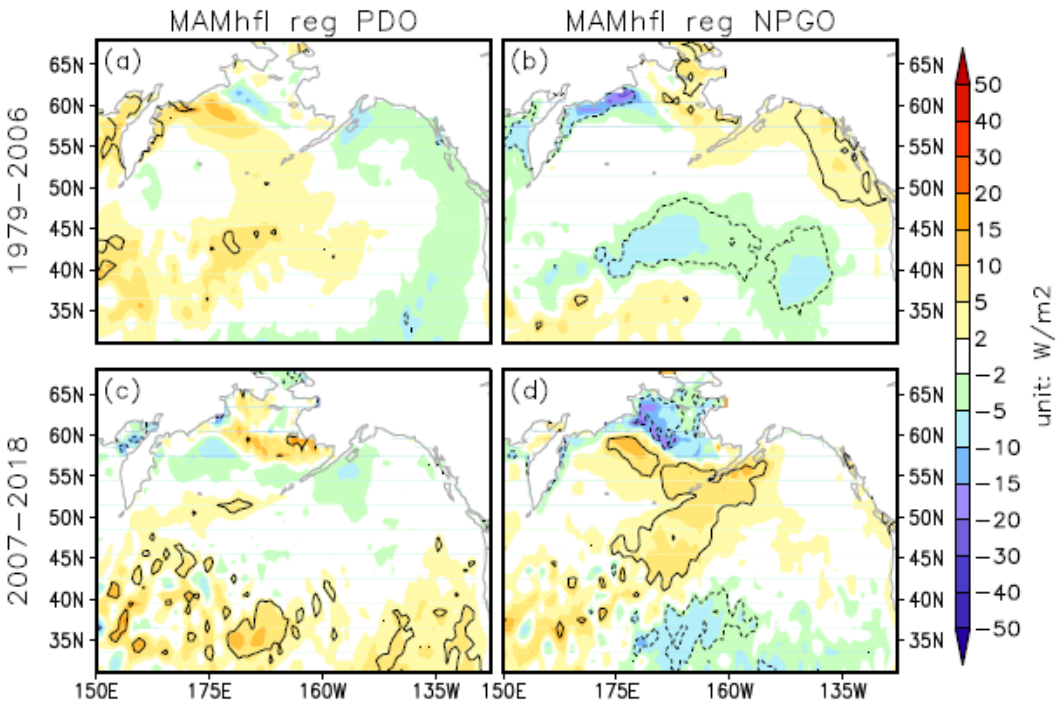

Figure 9. (a) & (b) Regression of March-May mean surface turbulent (sensible + latent) heat flux onto the PDO (left panels) and NPGO (right panels) indices during the period of 1979-2006. (c) & (d) Same as (a) & (b), but for the period of 2007-2018. Solid (dashed) lines enclose the positive (negative) regression coefficients that are significant at the 95% confidence level.

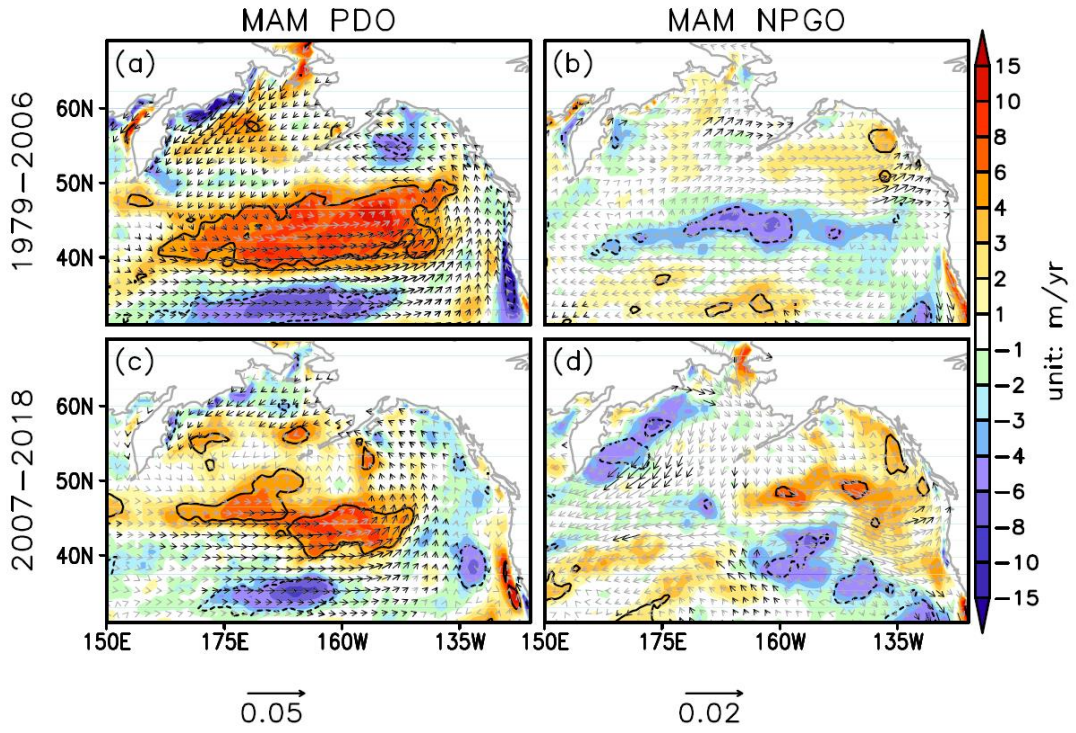

Figure 10. Same as Fig. 9, but for the regression of surface wind stress (vector) and Ekman pumping rate (color shading) anomalies. Solid (dashed) lines enclose the positive (negative) regression coefficients of Ekman pumping that are significant at the 95% confidence level. The black (gray) vectors indicate the wind stress regression coefficients are statistically significant (non-significant) at the 95% confidence level.

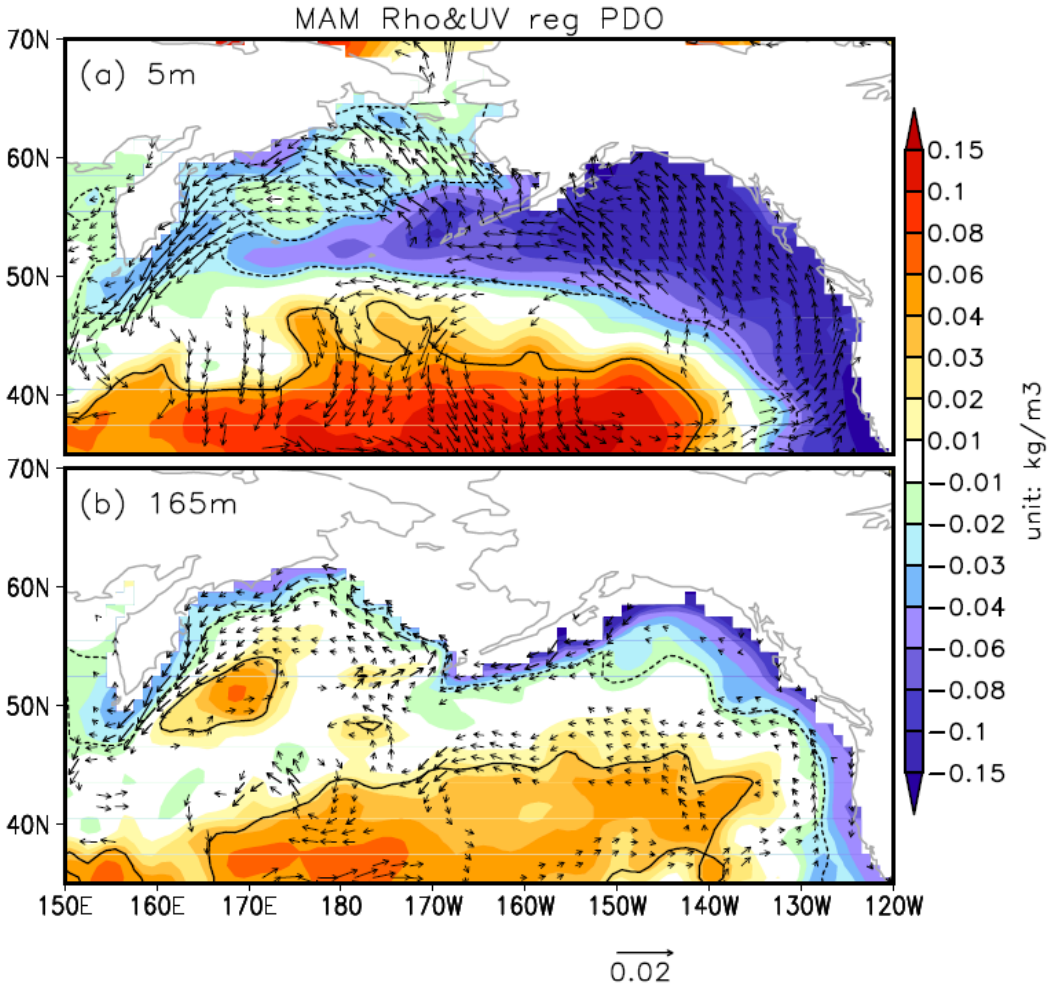

Figure 11. (a) Regressions of surface (5m) density (color shading) and zonal and meridional velocities (vector) onto the PDO index. Solid (dashed) lines enclose the positive (negative) density anomalies that are significant at the 95% confidence level. Only the velocity anomalies that are significant at the 95% confidence level are plotted. (b) Same as (a), but for the subsurface layer (165m).

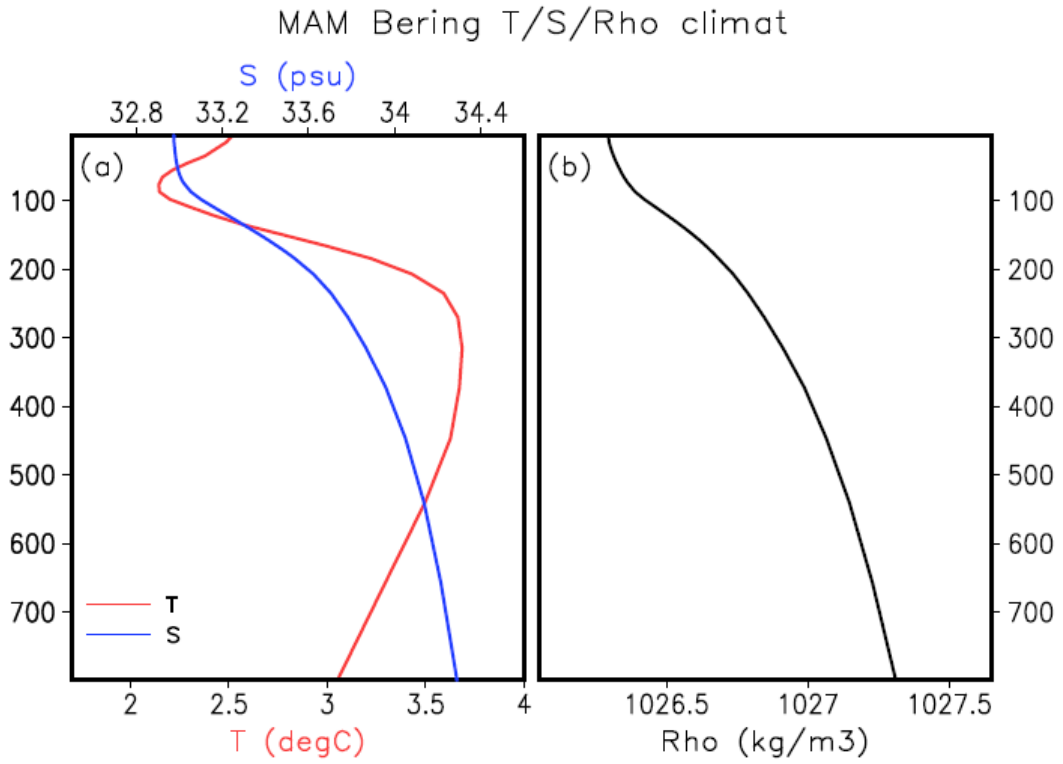

Figure 12. Climatological vertical profile of spring (March-May) Bering deep basin (160-190E, 50-60N) mean temperature and salinity (a) and density (b).

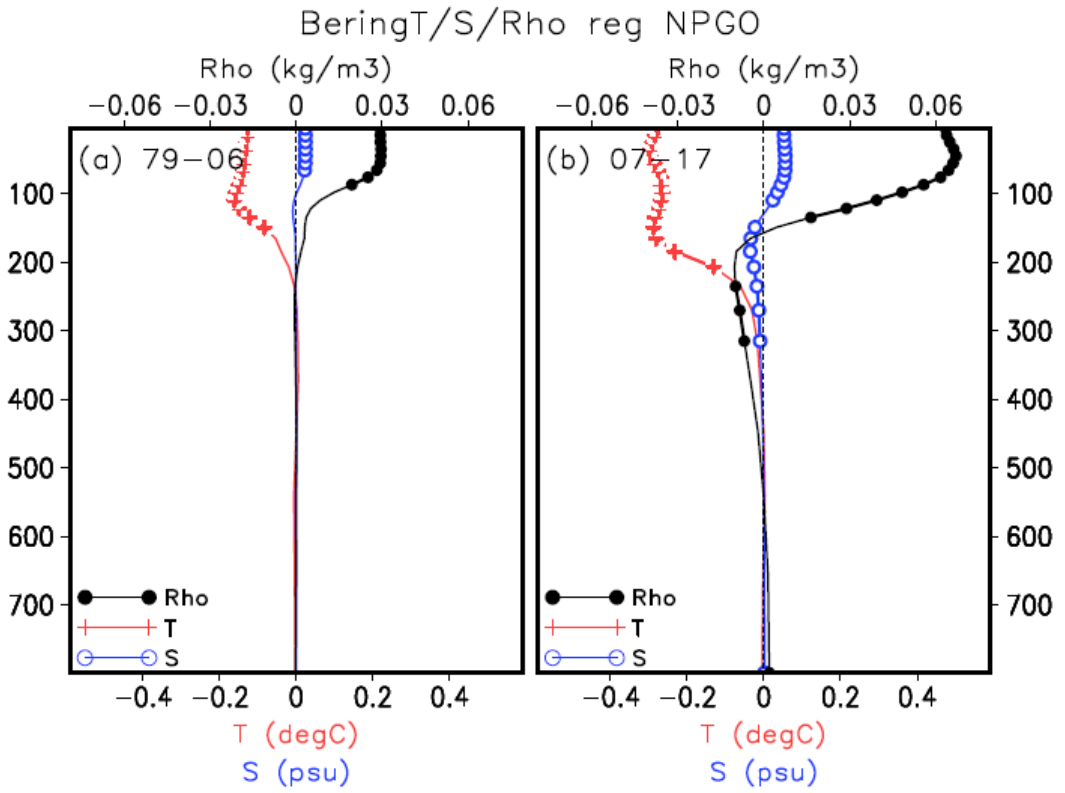

Figure 13. Regression of Spring (March-May mean) Bering deep basin temperature, salinity and density on the NPGO index during the 1979-2006 period (a) and the 2007-2017 period (b) for each depth layer. The marks of black dot, red cross and blue circle denote the regression coefficients that are significant at the 85% significant t test for density, temperature and salinity respectively.

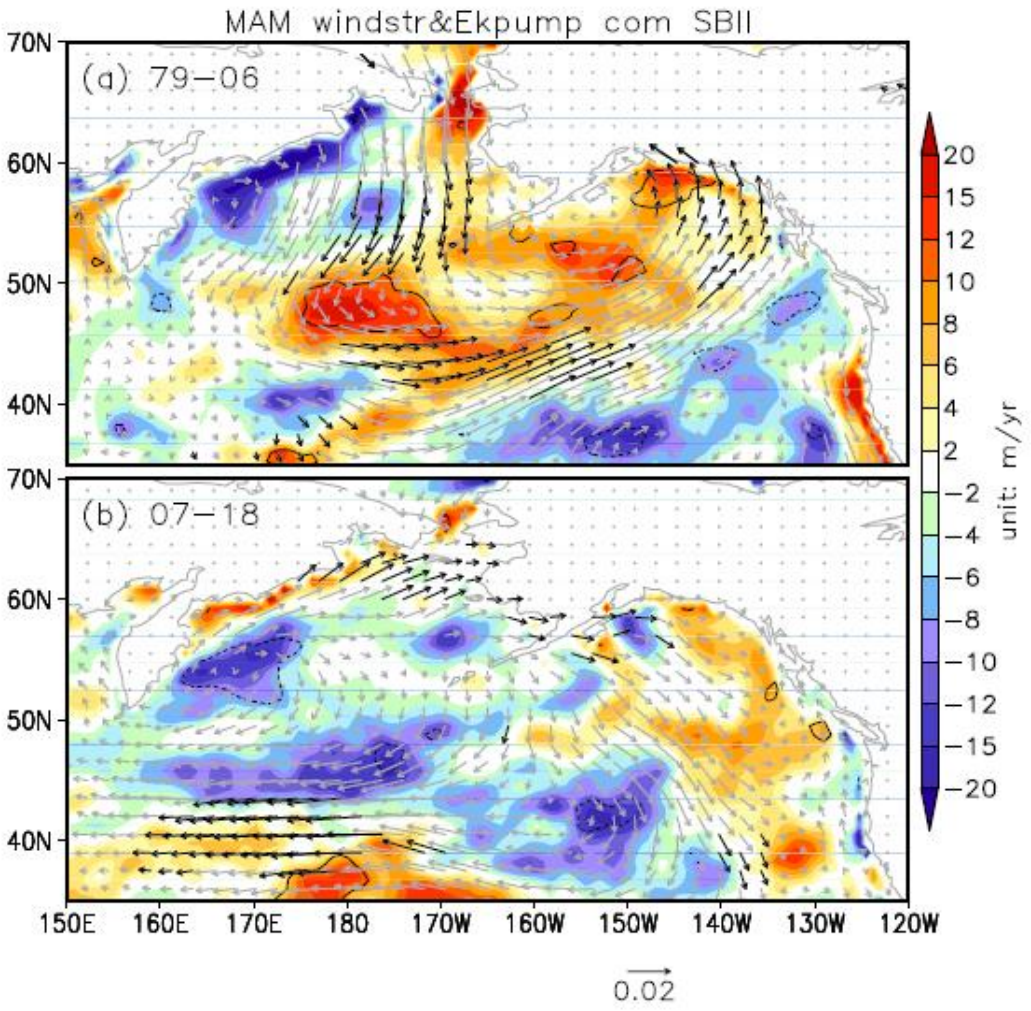

Figure 14. Composites of spring wind stress (vector) and Ekman pumping rate (color shading) based on the SBII high minus low index during the period of 1979-2006 (a) and the period of 2007-2018 (b).

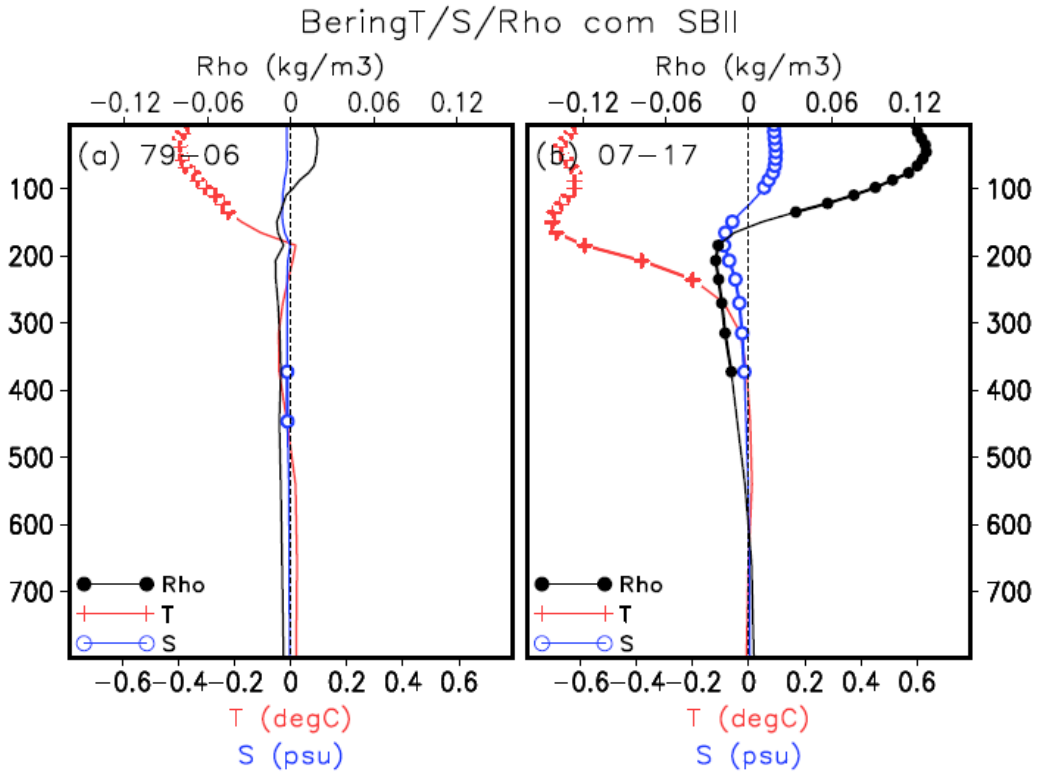

Figure 15. Composites of Spring (March-May mean) Bering deep basin temperature, salinity and density based on the SBII high minus low index during the 1979-2006 period (a) and the 2007-2017 period (b) for each depth layer. The marks of black dot, red cross and blue circle denote the regression coefficients that are significant at the 85% significant t test for density, temperature and salinity respectively.